JOURNAL OF GEOPHYSICAL RESEARCH, VOL. 99, NO. C9, PAGES 18,275–18,304, SEPTEMBER 15, 1994

Diapycnal mixing in western boundary currents

J. L. Pelegrí [1] and G. T. Csanady

Center for Coastal Physical Oceanography, Old Dominion University, Norfolk, Virginia

Abstract. In a previous study (Pelegrí and Csanady, 1991) we found upward entrainment and two-way exchange between the upper thermocline and surface layers of the Gulf Stream. Here we use isopycnic coordinates to analyze the mechanism of diapycnal shear-induced mixing in western boundary currents. A hydrographic section across the Gulf Stream off the Mid-Atlantic Bight is used for a case study. It shows that the upper thermocline layers of the Gulf Stream are characterized by relatively small (16 m averaged) gradient Richardson numbers, Ri. Analysis of the Jacobian, $J = \partial z/\partial \rho$ (with z the depth and ρ the potential density), total vorticity and potential vorticity fields shows that this region has low Jacobian values associated with high values of potential vorticity, as required theoretically for the case of dominant diapycnal mixing. The density tendency, $w_\rho = D\rho/Dt$, is calculated from the vertical gradient of the Reynolds density flux, the latter parameterized as density eddy diffusivity divided by the Jacobian. We use Munk and Anderson's (1948) expression for the eddy diffusivity coefficient, modified to conform to data of Ueda et al. (1981), maintaining a $Ri^{-3/2}$ dependence for large Ri. From this we obtain an explicit expression for w_ρ in terms of the Ri and J distributions. The distributions of w_ρ, its diapycnal gradient, $\partial w_\rho/\partial \rho$, and the diapycnal velocity, $w_d = Jw_\rho$, are then calculated. Regions of high diapycnal convergence (large negative $\partial w_\rho/\partial \rho$ values) coincide with the location of anomalously low Jacobians, in agreement with the idea that diapycnal mixing is the consequence of anomalies produced during frontogenesis in some phase of the meanders. We suggest that this process, taking place intermittently in space and time, is responsible for two-way exchange in western boundary currents.

1. Introduction

Analytical models of thermocline circulation due to *Rhines and Young* [1982], *Luyten et al.* [1983], and others have provided much insight into how the interior of subtropical gyres works. However, the dynamics of the crucial western end of these gyres remains obscure. The rise of the thermocline near the western boundary, the separation of the current from the coast, or its adjustment to the increasing planetary vorticity have not been fully accounted for. An understanding of the dissipation mechanisms involved is necessary to produce fully realistic models of the subtropical gyres. Apart from their crucial dynamical role, boundary currents transport a vast amount of heat poleward, as well as a large load of nutrients, two important factors in climate and in the global biogeochemical cycle. In this paper we examine diapycnal mixing and show that it is probably one of the important dissipation mechanisms in western boundary currents.

In a previous paper [*Pelegrí and Csanady*, 1991] (hereinafter PC) we analyzed water and nutrient transport along nine isopycnal layers in five hydrographic sections across the Gulf Stream. There we documented a nutrient stream associated with the upper thermocline layers of the Gulf Stream ($26.5 < \sigma_t < 27.3$), which transports some 10^3 kmol s^{-1} of nitrate and proportional amounts of other nutrients. A two-box model for the region between the Florida Straits and the Mid-Atlantic Bight showed inflow from the surface ($\sigma_t < 26.8$) and thermocline ($26.8 < \sigma_t < 27.5$) layers of the interior subtropical gyre at rates of 12 and 15 Sv, respectively. Additionally, we found significant upward entrainment and two-way exchange between these layers, both of about 2.4 Sv. These values correspond to overall upward entrainment and two-way exchange rates (per unit length of the stream) of about 1.6 m^2 s^{-1}, or mixing coefficients of 2×10^{-5} m s^{-1} over a stream 80 km wide.

From an analysis of data on the formation and disappearance of the Mid-Atlantic Bight slopewater pycnostad, *Csanady and Hamilton* [1988] estimated a mean

[1] Now at Facultad de Ciencias del Mar, Universidad de Las Palmas de Gran Canaria, Las Palmas de Gran Canaria, Canary Islands, Spain

Paper number 94JC01201.
0148-0227/94/94JC-01201$05.00

upwelling rate on the cyclonic side of the Gulf Stream of about 4 m^2 s^{-1} per unit length. *Csanady* [1989] related western boundary upwelling to energy dissipation in ocean gyres and postulated that it is effected through Reynolds mass flux (correlation between layer depth and cross-stream velocity). Our estimate in PC for the overall rate of upward entrainment plus two-way exchange between the upper thermocline and surface layers, 3.2 m^2 s^{-1}, is similar to *Csanady and Hamilton*'s [1988] estimate for western boundary upwelling. A connection between them seems likely: The supply for both upward entrainment and upwelling into the coastal waters must necessarily come from the upper thermocline layers, joining the Gulf Stream between the Florida Straits and the Mid-Atlantic Bight at a rate of some 10 m^2 s^{-1} per unit length.

Diapycnal mixing in western boundary currents has received little attention in the literature. *Gregg and Sanford* [1980] analyzed several profiles of temperature and velocity shear in the Gulf Stream and concluded that shear-induced mixing was possible, although they thought it was probably less important than thermohaline intrusions. *Stommel*'s [1965] early monograph on the Gulf Stream is the only reference, to our knowledge, where diapycnal mixing is considered as a likely phenomenon for the Gulf Stream. Talking in terms of the internal Froude number (the square of the inverse bulk Richardson number), he showed that a simple potential vorticity conserving model allows supercritical Froude numbers. Here we will endorse the concept that diapycnal mixing in the Gulf Stream may have local values high enough to modify the distribution of isopycnals height and other dynamical quantities, such as the isopycnic potential vorticity.

Isopycnic coordinates, with potential density ρ used as the vertical coordinate, are the natural framework for studying diapycnal mixing. In this framework we review the kinematics of diapycnal mixing and the equations of motion in isopycnic coordinates in the presence of diapycnal mixing. The Jacobian of the transformation from Cartesian to isopycnic coordinates, $J = \partial z/\partial \rho$, is an important parameter in this analysis. We investigate conditions necessary for the material tendency of the Jacobian, and for potential vorticity, to be controlled by diapycnal divergence/convergence.

The theory is tested with data from a Gulf Stream hydrographic section off the Mid-Atlantic Bight. We examine several pieces of evidence, such as the distribution of the Richardson number, indicative of shear mixing in the Gulf Stream. Next, we look at the distribution of the Jacobian, total vorticity, and potential vorticity in isopycnic coordinates. We show that the upper thermocline is the locus of low Jacobian values responsible for associated high values of potential vorticity. We argue that in these conditions diapycnal transfer is dominant, so that both the mass conservation and potential vorticity equations reduce to simple forms. Assuming that diapycnal transfer is the result of shear-induced small-scale instabilities, we relate it to the gradient Richardson number and the local Jacobian. We show that regions with small Jacobian (large potential vorticity) values imply large diapycnal convergence that tends to eliminate these anomalies. This leads us to the view that diapycnal mixing is the consequence of local anomalies produced during frontogenesis in Gulf Stream meanders. We end by comparing our results with analogous observations in the upper level atmospheric jet stream.

2. Density Tendency and Diapycnal Velocity

How do local instabilities and mixing develop? In this and the next section we seek an answer with the help of the mass, momentum, and vorticity equations in isopycnic coordinates, in the presence of diapycnal mass transfer. As a first step, in this section we will define what we mean by "time-mean" density surfaces and we will show how to estimate the corresponding diapycnal velocities. Before doing so, however, a few clarifications about terminology will follow.

In oceanographic literature "entrainment velocity" refers to the rate of vertical transfer across a sharp interface separating two layers of water (see reviews by *Turner* [1973, 1986] and *Fernando* [1991]). This nomenclature can be easily generalized to a continuously stratified flow, with transfer taking place between adjacent layers of different density, or isopycnal layers [e.g., *Csanady*, 1990]. *McDougall* [1984] initially introduced the concepts of "diapycnal" and "dianeutral velocities" as those normal to the isopycnal and neutral surfaces, respectively. In subsequent work, *McDougall* [1987a, b, 1988] redefined his system of reference in such a way that it is equivalent to the isopycnic (or isoneutral) system of reference, with lateral distances measured on the horizontal plane projection and motion through isopycnals (or neutral surfaces) being in the vertical direction; *McDougall* [1988] pointed out that the difference between the diapycnal velocity in the vertical direction and its value in the direction normal to the isopycnal is, in most cases, negligible. In the isopycnic reference system, however, it turns out that the definitions for entrainment velocity and diapycnal velocity are equivalent. Here because of the common usage of entrainment velocity for two-layer flow, we will follow the "diapycnal velocity" terminology.

The diapycnal velocity is indeed a velocity, i.e., it gives the material rate of change of position. In isopycnic coordinates it is convenient to introduce the material rate of change of density, which we will call "density tendency", and has units of density over time. (This name is anologous to "pressure tendency", sometimes employed in meteorology when using isobaric coordinates. An alternative choice would be "isopycnic vertical velocity", analogous to the meteorological language of "isobaric vertical velocity", but we will avoid it because it implies units of velocity. Still another possibility would be to use "diabatic density rate", similar to "diabatic heating rate" which is sometimes used in isentropic coordinates. This name, however, suggests that the density changes due to heating processes, which are only important in the atmosphere or uppermost ocean,

rather than due to actual cross-isopycnal mass transfer processes). We will show in this section that the density tendency and diapycnal velocity are directly related (through the Jacobian), as we should expect when considering that water entrained from one isopycnal layer into another must change its density.

In this paper we will ignore any differences between neutral and isopycnal surfaces. In our region of interest (the upper thermocline of western boundary currents) these differences are small due to the proximity of the (surface) reference pressure level and the relatively large stratification. An estimate for the difference between these surfaces across the Gulf Stream, obtained with the method suggested by *McDougall* [1987b, p. 1962], is of about 2 m. We will see that this height is much smaller than the relevant vertical scales for diapycnal mixing.

2.1. The "Mean" Density Tendency and Diapycnal Velocity

In the Cartesian (x, y, z) system, with velocity components (u, v, w), we can define the instantaneous density tendency as

$$w_\rho \equiv \frac{D\rho}{Dt} = \frac{\partial \rho}{\partial t} + u\frac{\partial \rho}{\partial x} + v\frac{\partial \rho}{\partial y} + w\frac{\partial \rho}{\partial z}, \qquad (1)$$

where $D/Dt \equiv \partial/\partial t + u\,\partial/\partial x + v\,\partial/\partial y + w\,\partial/\partial z$ is the material change operator in Cartesian coordinates.

The mass conservation equation in Cartesian coordinates is

$$\frac{\partial \rho}{\partial t} + \frac{\partial (u\rho)}{\partial x} + \frac{\partial (v\rho)}{\partial y} + \frac{\partial (w\rho)}{\partial z} = 0. \qquad (2)$$

In an incompressible fluid this equation is equivalent to $w_\rho = 0$.

It is reasonable to suppose that the timescale of instabilities developing in regions of significant mixing is much shorter than the timescale of significant displacements of the boundary current. Over the latter timescale, the fast unstable motions may be regarded as turbulence, giving rise to the conventional Reynolds fluxes of density. In this conceptual framework, the slowly changing "mean" density field $\tilde{\rho}$ is viewed as the stochastic average over a large number of realizations, or more practically, a time mean taken over the long-time scale. Fast motions distorting a given density isopleth, ρ, are removed by time-averaging the depths taken by that isopleth over the long-time scale, for each x and y, to give $\tilde{z} = z(x, y, \rho = \tilde{\rho})$.

With this conceptual model in mind, we decompose the density and velocity fields into fast (prime) and slow (tilde) motions: $\rho = \tilde{\rho} + \rho'$, $u = \tilde{u} + u'$, $v = \tilde{v} + v'$, $w = \tilde{w} + w'$. Taking the mean over the long-time scale, the mass conservation equation becomes

$$\begin{aligned} \tilde{w}_\rho &\equiv \frac{\partial \tilde{\rho}}{\partial t} + \tilde{u}\frac{\partial \tilde{\rho}}{\partial x} + \tilde{v}\frac{\partial \tilde{\rho}}{\partial y} + \tilde{w}\frac{\partial \tilde{\rho}}{\partial z} \\ \tilde{w}_\rho &= -\left[\left(\frac{\partial}{\partial x}(\overline{u'\rho'}) + \frac{\partial}{\partial y}(\overline{v'\rho'}) + \frac{\partial}{\partial z}(\overline{w'\rho'})\right]\right. \\ \tilde{w}_\rho &= -\nabla \cdot \tilde{\mathbf{F}}, \end{aligned} \qquad (3)$$

having assumed incompressibility. The (mean) turbulent density flux vector, or Reynolds density flux, has components $\tilde{\mathbf{F}} \equiv (\tilde{F}_x, \tilde{F}_y, \tilde{F}_z) \equiv (\overline{u'\rho'}, \overline{v'\rho'}, \overline{w'\rho'})$. In the atmosphere the vertical density flux may be due both to diabatic heating (latent heat release and radiation flux divergence) and mixing, but in the ocean (except in the uppermost 10 m or so) the contribution from diabatic heating (or cooling) is negligible.

The density tendency, w_ρ, defined in the isopycnic system (x, y, ρ), can be further related to the vertical velocity, w, in the vertical coordinate (x, y, z) system, as follows

$$w = \frac{\partial z}{\partial t} + u\frac{\partial z}{\partial x} + v\frac{\partial z}{\partial y} + w_\rho \frac{\partial z}{\partial \rho}. \qquad (4)$$

In the long-time mean systems, $z' = 0$ and $w_\rho = \tilde{w}_\rho$, so an equivalent relation holds

$$\begin{aligned} \tilde{w} &\equiv \frac{\mathcal{D}\tilde{z}}{\mathcal{D}t} = \frac{\partial \tilde{z}}{\partial t} + \tilde{u}\frac{\partial \tilde{z}}{\partial x} + \tilde{v}\frac{\partial \tilde{z}}{\partial y} + \tilde{w}_\rho \frac{\partial \tilde{z}}{\partial \tilde{\rho}} \\ \tilde{w} &= \frac{d\tilde{z}}{dt} + \tilde{w}_\rho \frac{\partial \tilde{z}}{\partial \tilde{\rho}} = \frac{d\tilde{z}}{dt} + \tilde{w}_d, \end{aligned} \qquad (5)$$

where $\mathcal{D}/\mathcal{D}t \equiv \partial/\partial t + \tilde{u}\,\partial/\partial x + \tilde{v}\,\partial/\partial y + \tilde{w}_\rho\,\partial/\partial\tilde{\rho}$, expresses the material change as seen from the long-time mean isopycnic coordinate system. The contributions to the mean vertical velocity are $d\tilde{z}/dt \equiv (\partial/\partial t + \tilde{u}\,\partial/\partial x + \tilde{v}\,\partial/\partial y)\,\tilde{z}$, which is the result of the local vertical motion of the mean isopycnals plus the vertical component of motion along these surfaces, and $\tilde{w}_d \equiv \tilde{w}_\rho \tilde{J} \equiv \tilde{w}_\rho\,\partial\tilde{z}/\partial\tilde{\rho}$, which is the mean diapycnal velocity. This last velocity is directly related with the mean density tendency (or Reynolds density flux divergence) through the mean Jacobian; physically, this may be interpreted as the rate of density change due to cross-isopycnal displacements in a "mean" density system of reference. Notice that (5) is the relation for the "entrainment velocity" commonly used in mixed-layer models [e.g., *deSzoeke*, 1980; *Csanady*, 1989, 1990]; for steady state it corresponds to (10) in *McDougall* [1988].

Hereinafter, except where indicated, the isopycnal surfaces and diapycnal velocities will always correspond to the above discussed "mean" values (for clarity, henceforth we drop tildes). Additionally, and since we are doing our analysis in isopycnic coordinates, we will refer to the vertical isopycnic gradient simply as a diapycnal gradient and to any along-isopycnal gradient as an epipycnal gradient. In particular, we will call diapycnal shear to the diapycnal gradient of the horizontal velocity, $\partial v/\partial\rho$, and diapycnal divergence (convergence) to the diapycnal gradient of the density tendency, $\partial w_\rho/\partial\rho$. Finally, when referring to "overall" quantities, a much longer time average (over many long-time scales) will be implied.

2.2. Estimating the Density Tendency

In connection with surface mixed-layer deepening, a plethora of models have been proposed in the literature for calculating the diapycnal (or entrainment) velocity (see reviews by *Zilitinkevich et al.* [1979], *Deardorff*

[1983], *Gaspar* [1988], and *Fernando* [1991]). In these models w_d is often calculated from the buoyancy flux term in the turbulence kinetic energy equation. The leading terms in that equation are turbulent energy production and dissipation, while the buoyancy flux is typically about 3% of these terms. A relatively small error in the prediction of the leading terms therefore translates into a large error for the buoyancy flux, and for the diapycnal velocities. *Fernando* [1991] summarized laboratory and field data on entrainment in stratified shear flows and showed that the observations do not support the models.

Our results in PC pointed at the existence of two processes responsible for overall water exchange between the upper thermocline and surface strata of the Gulf Stream. The first process, upward entrainment, is responsible for the transfer of water and properties from the upper thermocline into the surface stratum. The second process, two-way exchange between both strata, has no net mass transfer but it has net exchange of properties. The density tendency, which must be responsible for both processes, may be expressed as the divergence of the Reynolds density flux (equation (3)). The preponderance of one process or another is the result of the temporal and spatial variation of the Reynolds density flux.

The Reynolds density flux vector, **F**, is perpendicular to the "mean" isopycnals. The relatively small slope of the isopycnals allows us to approximate **F** by its vertical component, $F_z = \overline{w'\rho'}$, and its divergence by $\nabla \cdot \mathbf{F} \simeq \partial F_z/\partial z$. With this approximation we can make estimates of the density tendency using a first-order closure model similar to *Munk and Anderson*'s [1948]. F_z is parameterized using a spatially varying vertical density eddy diffusivity, K:

$$F_z = -K\frac{\partial \rho}{\partial z} = -\frac{K}{J}. \tag{6}$$

Therefore (3) becomes

$$w_\rho \simeq -\frac{\partial F_z}{\partial z} = \frac{\partial}{\partial z}\left(\frac{K}{J}\right)$$

$$w_\rho \simeq \frac{1}{J}\frac{\partial K}{\partial z} + K\frac{\partial^2 \rho}{\partial z^2} = \frac{1}{J^2}\frac{\partial K}{\partial \rho} - \frac{K}{J^3}\frac{\partial J}{\partial \rho}. \tag{7}$$

The diapycnal velocity is related to the density tendency by $w_d = J w_\rho$ (equation (5)).

This expression may be compared with *McDougall*'s [1988, equation (70)] result for the diapycnal velocity in a "neutral" reference system. McDougall's expression contains a number of additional terms arising from thermobaricity and cabbeling, plus epineutral mixing. For relatively shallow neutral surfaces in the North Atlantic, at levels of about 600 m, *McDougall* [1987a] estimated the joint effect of thermobaricity and cabbeling to be of -0.2×10^{-7} m s^{-1}. These contributions are neglected by comparison with the estimates obtained in section 4.3 using (7). Additionally, the small differences between neutral and isopycnal surfaces in the upper thermocline of the Gulf Stream allows us to neglect any epineutral contribution, to the same order of accuracy with which we omit the epipycnal Reynolds density fluxes.

McDougall's [1988] expression for the diapycnal velocity still contains two additional nonlinear terms, $K(\hat{\alpha}\,\theta_{zz} - \hat{\beta} S_{zz})$, where subindexes indicate derivatives, θ is potential temperature, S is salinity, and $\hat{\alpha}$ and $\hat{\beta}$ are the thermal expansion and saline contraction coefficients evaluated at the reference pressure $p = p_r$. Following *McDougall and You* [1990, equation (17)], we can take account of these contributions and approximate the equation for the density tendency as

$$w_\rho = \frac{w_d}{J} \simeq \frac{\partial}{\partial z}\left(\frac{K}{J}\right) + \rho K \frac{\partial \hat{\alpha}}{\partial \theta}\left(\frac{\partial \theta}{\partial z}\right)^2. \tag{8}$$

where we have ignored the cabbeling and thermobaric terms, as well as any epineutral fluxes. *McDougall and You* [1990] showed that the contribution of the last term in (8) may be important in much of the Atlantic Ocean. We may estimate the maximum contribution of this term using $\partial \hat{\alpha}/\partial \theta \simeq 10^{-5}$°C^{-2}, and the following maximum values from our case study (a hydrographic section across the Gulf Stream): $\partial \theta/\partial z \sim 10^{-2}$ - 10^{-1} °C m^{-1} (see Figures 3 and 14) and $K \simeq 10^{-5}$ m^2 s^{-1} (section 4.1). This gives a value of 10^{-10} - 10^{-9} kg m^{-3} s^{-1}, which is several times smaller than the maximum contribution from the term retained in (7) (section 4.3), and it will be neglected.

Equation (7) shows that the density tendency may be thought of as arising from two terms: the vertical variation of eddy diffusivity and uneven vertical distances between isopycnals equally spaced in σ_θ space. The first term generates a density tendency in the direction of decreasing K (recall that J is negative), or equivalently, a diapycnal velocity in the direction of increasing K (as discussed further by *Csanady* [1990]). This agrees with the empirical findings that entrainment takes place in the direction of increasing turbulence [*Turner*, 1973, 1986]. The second contribution, which depends linearly on K, is due to continuity of vertical mass transfer, and differs from zero whenever the Jacobian changes with depth.

Gargett [1984] reviewed the various methods employed in the literature to estimate K and concluded that the most accurate and consistent representation portrays K as a decreasing function of the Vaisala frequency, N [$N^2 = (g/\rho)(\partial \rho/\partial z) = g/(\rho J)$]. *Sarmiento et al.* [1976], using radon profiles near the ocean floor, estimated K to be inversely proportional to N. *Svensson* [1980], using budget models with conservative tracers for a wide variety of estuarine and oceanic situations, estimated this dependence to be $K \propto N^{-1.2}$. *Armi* [1979] examined the effects of epipycnal gradients on eddy diffusivity in a vertical advective-diffusive equation for density. He pointed out that the epipycnal gradients in K play the role of a horizontal advective velocity and used the assumptions of dominant boundary mixing and zero vertical velocity to obtain a dependence of the form $K \propto N^{-2}$. This result showed good agreement with observations at middepths. We note that such a rela-

tionship between K and N arises directly from (7) for the case of zero diapycnal velocity (no vertical gradients in $\overline{w'\rho'}$). This situation is to be expected at middepths in the ocean, away from sources or sinks of turbulence, and for negligible shear. In this case (7) becomes

$$\frac{1}{K}\frac{\partial K}{\partial \rho} - \frac{1}{J}\frac{\partial J}{\partial \rho} = 0, \tag{9}$$

which results in Armi's dependence,

$$K = cJ = \frac{cg}{\rho N^2}, \tag{10}$$

where c is a constant of integration.

A dependence of K on N alone may only be valid for oceanic regions with negligible shear. In general, K will depend both on external sources of turbulence and on the dynamical stability of the flow. To model shear-induced instability in stratified flow, the eddy diffusivity is expressed in terms of the (gradient) Richardson number, Ri. In the meteorological literature there have been many suggestions of such a functional form for K. In oceanography, one early ansatz was *Munk and Anderson*'s [1948] relationship of the form $K = K_0(1 + \beta Ri)^{-3/2}$, with $\beta = 10/3$, and K_0 the density eddy diffusivity in neutral conditions. In the late 1970s, studies by *James* [1977, 1978], *Kao et al.* [1977], *Hamilton and Rattray* [1978], and *Foo* [1981] all employed this kind of parameterization.

From the depth and geostrophic velocity distributions we can estimate Ri as follows:

$$Ri = \frac{g\frac{\partial \rho}{\partial z}}{\rho\left(\frac{\partial v}{\partial z}\right)^2} = \frac{gJ}{\rho\left(\frac{\partial v}{\partial \rho}\right)^2}. \tag{11}$$

A number of theoretical investigations have shown the existence of a critical Ri value, Ri_c, below which mixing is supposed to develop. The value of Ri_c depends on the flow under consideration but ranges from zero to 0.25, the latter value applying to unbounded parallel shear flow (for reviews see *Miles* [1986] and *Fernando* [1991]). Our case study (section 4) will show an example where Ri attains a minimum in the upper thermocline layers of the Gulf Stream and will suggest the likelihood of small-scale turbulence developing due to hydrodynamic instability in stratified shear flow.

The first equality in (11) defines Ri in Cartesian coordinates, the second its equivalent in isopycnic coordinates. The second definition shows that Ri diminishes with J (isopycnals close together) and with increasing diapycnal shear. This is contrary to the intuitive idea that Ri should increase with stratification (decreasing J). The key factor is the velocity gradient: if the diapycnal shear remains constant the Richardson number will decrease with increasing stratification.

Peters et al. [1988], in a study of the equatorial undercurrent (where the shear is strong), found two different regimes of K dependence on Ri. In the low Ri regime ($Ri < 0.3$), they found a nearly catastrophic decrease of K with Ri ($K \sim Ri^{-9}$). Such a relation is very appealing because it conforms to the theoretical critical Ri criterion. At higher Ri their $K(Ri)$ dependence closely resembles the Munk-Anderson formula. The work of *Peters et al.* [1988] is a remarkable pioneering investigation, but the authors warn that their indirect method of flux determination undermines the accuracy of the results.

For stratified flows with strong shear the comprehensive empirical study by *Ueda et al.* [1981] seems to offer a good basis for specifying the $K(Ri)$ relationship. Ueda et al. used observations in the atmospheric boundary layer above the surface layer, as well as data of *Komori et al.* [1983] for stratified open-channel flow. Figure 1, modified from *Ueda et al.* [1981], shows the variation of the ratio K_H/K_{H0} with Ri, where K_H is the heat diffusivity and K_{H0} is the heat diffusivity in neutral conditions. The data points are from direct measurements in the atmospheric boundary layer, the different symbols indicating the distance above the surface. The dotted line represents an interpolation formula derived by *Ueda et al.* [1981] from the laboratory data of *Komori et al.* [1983]. The formula is a modification of *Ellison*'s [1957] suggestion for the relation between vertical eddy diffusivity and eddy viscosity. *Ueda et al.* [1981] state that their results are consistent with *Deardorff*'s [1967], taken far from the surface, where direct boundary effects are not important.

Ueda et al. [1981] suggest that for large Ri the ratio K_H/K_{H0} decreases approximately as Ri^{-2}. However, we have plotted over this figure *Munk and Anderson*'s [1948] relation, both with $\beta = 10/3$ (dashed line), as they suggested, and with $\beta = 10$ (solid line). The $\beta = 10/3$ value indeed gives too small a decrease of the ratio K_H/K_{H0} with Ri, but the value $\beta = 10$ gives an approximation to the data which is as good as the one proposed by *Ueda et al.* [1981]. Since considerable evidence indicates that for large Ri the eddy diffusivity should decrease as $Ri^{-3/2}$ [*Turner*, 1986], we have chosen this Ri dependence. Hence assuming that the heat and salt eddy diffusivity are the same and equal to the density eddy diffusivity K, we obtain the following parameterization in terms of Ri and the density eddy diffusivity in neutral conditions K_0:

$$K = K_0(1 + 10Ri)^{-3/2}. \tag{12}$$

With this result, (7) for the density tendency becomes

$$w_\rho = \frac{-K_0}{J^3(1 + 10Ri)^{3/2}}\left[\frac{15J}{(1 + 10Ri)}\frac{\partial Ri}{\partial \rho} + \frac{\partial J}{\partial \rho}\right]. \tag{13}$$

We now need an estimate for K_0. In their pioneering study, *Munk and Anderson* [1948] employed unrealistically high K_0 values, as large as 0.1 $m^2\ s^{-1}$. A great deal of variation, however, still characterizes K values recently reported in the literature. Review papers by *Moum and Osborn* [1986], *Eriksen* [1987], *Gibson* [1987] and *Gregg* [1987] quote K values ranging from 10^{-6} to 10^{-4} $m^2\ s^{-1}$. *Hopfinger* [1987], in another review, has the upper bound as 10^{-3} $m^2\ s^{-1}$.

Gregg and Sanford [1980] estimated maximum K values consistently below 10^{-4} $m^2\ s^{-1}$ for the Sargasso Sea,

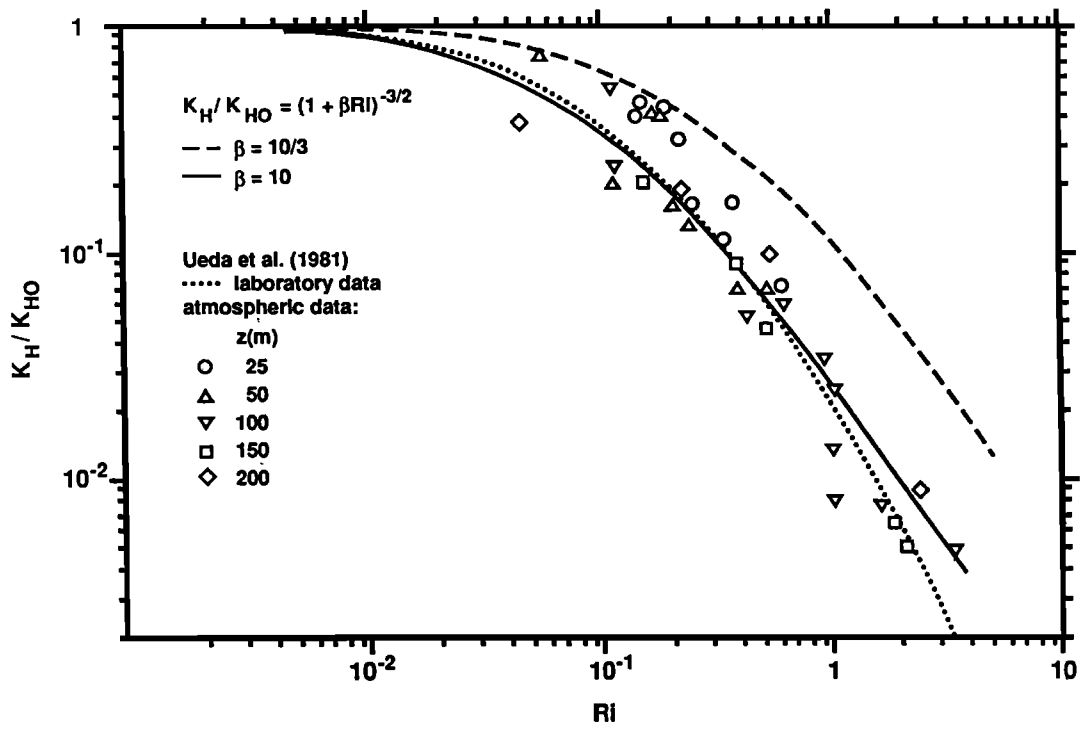

Figure 1. Variation of the ratio K_H/K_{H0} with Richardson number. Data reported by *Ueda et al.* [1981] for the atmospheric boundary layer are shown. The dotted line is *Ueda et al.*'s [1981] interpolation formula for laboratory data of *Komori et al.* [1983]. The dashed and solid lines correspond to *Munk and Anderson*'s [1948] expression with $\beta = 10/3$ and 10, respectively.

and one order of magnitude smaller in the Gulf Stream. *Hogg et al.* [1982] obtained, for the deep ocean, $K \simeq 3 - 4 \times 10^{-4}$ m^2 s^{-1}. *Lietzke and Lerman* [1975] and *Smethie* [1980], for small embayments, found $K \simeq 4 \times 10^{-4}$ m^2 s^{-1}. *Gargett* [1984] summarized a number of studies that give values as large as 10^{-3} m^2 s^{-1}. However, her best estimate was $K \simeq 2 - 3 \times 10^{-4}$ m^2 s^{-1}, for the depth range of 4 - 5 km.

The eddy diffusivity at *Ri*-critical conditions has to be close to the maximum K values reported. Accordingly, we have chosen $K_0 = 2.6 \times 10^{-3}$ m^2 s^{-1}. Using this value in (12) we obtain $K(Ri = 0.25) = 4 \times 10^{-4}$ m^2 s^{-1}.

3. Isopycnic Equations With Diapycnal Mixing

We consider now the governing equations in isopycnic coordinates, in the presence of a mean density tendency, w_ρ. A standard reference from the meteorological literature is *Dutton*'s [1976], who discussed some of these equations in isentropic coordinates. Other important works are *Bleck*'s [1978, 1979, 1985] and *Johnson*'s [1980] analyses in generalized coordinates. In the last two decades Rainier Bleck and his collaborators have discussed and numerically solved the governing equations for a number of oceanographic applications [e.g., *Bleck and Boudra*, 1986; *Bleck et al.*, 1988]). To the authors' knowledge, however, there is no comprehensive analysis on the possible role of density tendency in an isopycnic coordinate system of reference. This absence, we believe, warrants the space dedicated to the following analysis. We will show that large enough diapycnal convergence or divergence can control the separation between isopycnal layers, drive the potential vorticity balance, and cause instability and mixing.

3.1. Mass and Momentum Equations

To obtain the dynamical equations, we write down the mass and momentum balances in a fluid element of sides dx, dy and $Jd\rho$. Consistency with the discussion in section 2.1 dictates the use of "mean" isopycnals, but according to our convention there we have dropped tildes. The resulting equations are

$$\frac{\partial(Ju)}{\partial t} + \frac{\partial(Ju^2)}{\partial x} + \frac{\partial(Juv)}{\partial y} + \frac{1}{\rho}\frac{\partial(\rho Juw_\rho)}{\partial \rho} - fJv = -\frac{1}{\rho}[\frac{\partial(Jp)}{\partial x} + \frac{\partial}{\partial \rho}(p\frac{\partial z}{\partial x})] + JA, \quad (14)$$

$$\frac{\partial(Jv)}{\partial t} + \frac{\partial(Juv)}{\partial x} + \frac{\partial(Jv^2)}{\partial y} + \frac{1}{\rho}\frac{\partial(\rho Jvw_\rho)}{\partial \rho} + fJu = -\frac{1}{\rho}[\frac{\partial(Jp)}{\partial y} + \frac{\partial}{\partial \rho}(p\frac{\partial z}{\partial y})] + JB, \quad (15)$$

$$\frac{\partial p}{\partial \rho} + \rho J g = 0, \quad (16)$$

$$\frac{\partial J}{\partial t}+\frac{\partial (Ju)}{\partial x}+\frac{\partial (Jv)}{\partial y}+\frac{1}{\rho}\frac{\partial (\rho J w_\rho)}{\partial \rho} = C. \quad (17)$$

A and B are the resultant horizontal components of all dissipative forces, including Reynolds stresses and molecular friction, and C is the result of the horizontal Reynolds mass fluxes. In these equations all derivatives are taken along isopycnals, i.e., with the density ρ constant. Equations (14) and (15) are the horizontal momentum equations, (16) is the hydrostatic equation, and (17) is the mass conservation equation. These equations differ from the nondiffusive case [*Csanady*, 1989] due to the presence of terms A and B, and of those containing w_ρ.

Dividing through by J and using the mass conservation equation, the horizontal momentum balances can be rewritten in their "acceleration" form as

$$\frac{du}{dt}+w_\rho\frac{\partial u}{\partial \rho}-fv=-\frac{\partial \phi}{\partial x}+A, \quad (18)$$

$$\frac{dv}{dt}+w_\rho\frac{\partial v}{\partial \rho}+fu=-\frac{\partial \phi}{\partial y}+B, \quad (19)$$

with the potential ϕ defined as

$$\phi=\frac{p}{\rho}+gz. \quad (20)$$

Following common usage ϕ will be called the Montgomery potential, despite it is not the potential originally derived by *Montgomery* [1937] in a specific volume anomaly surface. As a reviewer pointed out, ϕ is an exact stream function for the geostrophic velocity only along in situ density surfaces (recall that ρ stands for potential density and isopycnals are surfaces of constant ρ). *McDougall* [1989] and *Zhang and Hogg* [1992] have shown that there are no exact stream functions in isopycnals and that the utilization of ϕ on these surfaces may lead to significant errors in the determination of the geostrophic velocity. In this study, however, we are not interested on the accurate determination of alongstream geostrophic velocities; instead, we are concerned in getting good estimates of their epipycnal and diapycnal gradients. In Appendix A we show that the above potential is adequate for these purposes.

The mass conservation equation (17) may be rewritten as the material tendency of $j=\rho J$,

$$\frac{\mathcal{D}j}{\mathcal{D}t}=-j\left(\frac{\partial u}{\partial x}+\frac{\partial v}{\partial y}\right)-j\frac{\partial w_\rho}{\partial \rho}+\rho C, \quad (21)$$

where $\mathcal{D}/\mathcal{D}t$ is the material derivative in isopycnic coordinates, as defined in (5). This relation shows that j, which is proportional to the separation between adjacent isopycnals, changes due to convergence (or divergence) of the flow in the epipycnal and diapycnal directions. If epipycnal convergence and horizontal Reynolds mass flux can be neglected (Appendix B), (21) reduces to

$$\frac{1}{j}\frac{\mathcal{D}j}{\mathcal{D}t}\simeq-\frac{\partial w_\rho}{\partial \rho}. \quad (22)$$

3.2. Vorticity Balance

The vorticity equation in isopycnic coordinates, derived from the cross product of the acceleration form of the momentum equations, may be written as

$$\frac{\partial \zeta}{\partial t}+\frac{\partial [u(\zeta+f)]}{\partial x}+\frac{\partial [v(\zeta+f)]}{\partial y}=S, \quad (23)$$

where $\zeta=\partial v/\partial x-\partial u/\partial y$ is the diapycnal (or vertical isopycnic) component of the relative vorticity (the difference between this and the vertical component being that here the derivatives are taken along isopycnals). The source term, S, is given by

$$\begin{aligned} S &\equiv \frac{\partial}{\partial x}\left(B-w_\rho\frac{\partial v}{\partial \rho}\right)+\frac{\partial}{\partial y}\left(w_\rho\frac{\partial u}{\partial \rho}-A\right) \\ S &= \left(\frac{\partial w_\rho}{\partial y}\frac{\partial u}{\partial \rho}-\frac{\partial w_\rho}{\partial x}\frac{\partial v}{\partial \rho}\right)+\left(\frac{\partial B}{\partial x}-\frac{\partial A}{\partial y}\right)-w_\rho\frac{\partial \zeta}{\partial \rho} \\ S &= T_i+T_o-w_\rho\frac{\partial \zeta}{\partial \rho}, \end{aligned} \quad (24)$$

where $T_i\equiv(\partial w_\rho/\partial y)(\partial u/\partial \rho)-(\partial w_\rho/\partial x)(\partial v/\partial \rho)$ and $T_o\equiv \partial B/\partial x-\partial A/\partial y$.

Following *Dutton* [1976, p. 341], T_i may be interpreted as tilting of horizontal vorticity by writing

$$\begin{aligned} \frac{\partial w_\rho}{\partial y}\frac{\partial u}{\partial \rho} &= \frac{\partial w_\rho}{\partial y}\left(\eta+\frac{\partial w_\rho}{\partial x}\right), \\ \frac{\partial w_\rho}{\partial x}\frac{\partial v}{\partial \rho} &= \frac{\partial w_\rho}{\partial x}\left(\frac{\partial w_\rho}{\partial y}-\xi\right), \end{aligned} \quad (25)$$

where η and ξ are the horizontal components of relative vorticity in isopycnic coordinates, $\xi=\partial w_\rho/\partial y-\partial v/\partial \rho$ and $\eta=\partial u/\partial \rho-\partial w_\rho/\partial x$. Hence T_i can be rewritten as

$$T_i=\left(\frac{\partial w_\rho}{\partial y}\frac{\partial u}{\partial \rho}-\frac{\partial w_\rho}{\partial x}\frac{\partial v}{\partial \rho}\right)=\left(\eta\frac{\partial w_\rho}{\partial y}+\xi\frac{\partial w_\rho}{\partial x}\right). \quad (26)$$

This shows that in the presence of epipycnal gradients of w_ρ, the horizontal relative vorticities, ξ and η, are converted into relative diapycnal vorticity, ζ.

With this partition, (23) and (24) reveal that changes in the vorticity on an isopycnal are caused by tilting of horizontal relative vorticity, T_i, torque by eddy stresses, T_o, and diapycnal advection of vorticity, $w_\rho\,\partial\zeta/\partial\rho$. An alternative form for these equations may be obtained by adding the diapycnal advection term to the local change and epipycnal advection terms. Then we obtain a vorticity tendency equation in the (x,y,ρ) system

$$\frac{\mathcal{D}(\zeta+f)}{\mathcal{D}t}=-(f+\zeta)\left(\frac{\partial u}{\partial x}+\frac{\partial v}{\partial y}\right)+T_i+T_o. \quad (27)$$

This tells us that the material change of the absolute vorticity is due to epipycnal convergence or divergence, tilting of horizontal vorticity and torque by eddy stresses.

Equation (23) may also be written as a flux potential vorticity equation

$$\frac{\partial (jq)}{\partial t}+\frac{\partial (ujq)}{\partial x}+\frac{\partial (vjq)}{\partial y}=T_i+T_o-w_\rho\frac{\partial \zeta}{\partial \rho}, \quad (28)$$

with the potential vorticity q defined as

$$q = \frac{\zeta + f}{j} . \tag{29}$$

The implications of this equation, for the behavior of q as a tracer, have been discussed by *Haynes and McIntyre* [1987, 1990]. Since the terms on the right-hand side of (28) may be written as the epipycnal divergence of a source term (equation (24)), they argued that the amount of q between adjacent isopycnals, or "potential vorticity substance" jq, can only change through epipycnal transport. However, as Haynes and McIntyre point out, q itself may change due to dilution or concentration of potential vorticity substance through diapycnal mass transfer.

For the analysis of data it is convenient to use the potential vorticity tendency equation. With the help of (17), the vorticity equation (23) may be transformed into

$$\frac{dq}{dt} = \frac{S}{j} + \frac{q}{j}\frac{\partial (j w_\rho)}{\partial \rho} , \tag{30}$$

or, equivalently, as the material tendency of potential vorticity in the (x, y, ρ) system

$$\frac{\mathcal{D}q}{\mathcal{D}t} = \frac{T_i}{j} + \frac{T_o}{j} + q\frac{\partial w_\rho}{\partial \rho} . \tag{31}$$

In neither of these two expressions does the right-hand side have the form of an epipycnal divergence, meaning that q may indeed change through processes other than epipycnal transport. In particular, the last equation tells us that the potential vorticity of a fluid parcel changes not only due to tilting of horizontal vorticity and torque by eddy stresses, but also due to diapycnal transfer associated with diapycnal divergence (or convergence). If T_i/j and T_o/j are relatively small (Appendix B), (31) may be approximated by

$$\frac{1}{q}\frac{\mathcal{D}q}{\mathcal{D}t} \simeq \frac{\partial w_\rho}{\partial \rho} . \tag{32}$$

Equations (21) and (31) give the material rates of change of j and q. If we were to examine the temporal change in properties on an isopycnal horizon, we would have to separate the contribution from diapycnal advection, i.e., $\mathcal{D}/\mathcal{D}t = d/dt + w_\rho \partial/\partial\rho$. In this manner we could follow a quasi-Lagrangian approach, with diapycnal advection becoming an additional term on the right-hand side of (21) and (31). However, when looking at the distribution of a tracer in one single (x, ρ) hydrographic section, we can only examine the existence of anomalies but we cannot differentiate whether these anomalies are produced following water particles that cross "mean" isopycnals (fully Lagrangian approach), following water parcels along isopycnal horizons (quasi-Lagrangian approach), or simply looking at local changes in time. In this case the approach is chosen depending on the physical mechanism we wish to study. Equations (21) and (31) use the full-Lagrangian approach to examine the creation of tracer (Jacobian and potential vorticity) anomalies through diapycnal convergence/divergence. This is in agreement with the fact that diapycnal advection alone (the additional term in the quasi-Lagrangian approach) cannot produce anomalies in the (x, ρ) plane, it can only advect them.

Equations (21) and (31) may be related, through the definition of potential vorticity, as follows

$$\frac{1}{q}\frac{\mathcal{D}q}{\mathcal{D}t} = -\frac{1}{j}\frac{\mathcal{D}j}{\mathcal{D}t} + \frac{1}{(\zeta + f)}\frac{\mathcal{D}(\zeta + f)}{\mathcal{D}t} \tag{33}$$

This equation states that the relative change in potential vorticity is due to contributions from relative changes in both j and $\zeta + f$. If diapycnal mixing is locally dominant then we should be able to use the approximations (22) and (32) for the left-hand side and the first term of the right-hand side, respectively. Hence for these approximations to be correct we require the contribution from the relative change in absolute vorticity in (33) to be small compared with the contribution from the relative change in j. In the next section we will examine the distribution of anomalies in a hydrographic section across the Gulf Stream. These anomalies, which we ascribe to material rates of change, will be compared with the anomalies in $\partial w_\rho/\partial\rho$, in order to infer the locations where diapycnal mixing is dominant.

4. Case Study

For our analysis we have examined one hydrographic section used in PC, across the Gulf Stream off the Mid-Atlantic Bight (see Figure 2), for which we have both nutrient and high resolution conductivity-temperature-depth (CTD) data (provided in processed and verified form by Mike McCartney of Woods Hole Oceanographic Institution (WHOI)). This section, referred to as section 36N, was occupied between June 12 and June 14, 1981, moving in the offshore direction. Figure 2 (adapted from originals courtesy of Jenifer Clark of the National Oceanic and Atmospheric Administration (NOAA)), shows two Gulf Stream frontal analysis maps made over the region of consideration just before (June 10, 1981) and after (June 15, 1981) section 36N was taken. These maps evidence the passage of a meander, specifically the region between its trough and crest, over the location of section 36N.

In order to use isopycnic coordinates, the CTD data, provided to us as average values over 2 m depth intervals, were smoothed with a running filter to 16 m interval averages. This was the minimum smoothing necessary to remove all potential density inversions in the data. Subsequently, levels of sigma-theta surfaces separated by 0.01 intervals were determined by cubic-spline interpolation. Figure 3 shows the 2-m-averaged original salinity, temperature and sigma-theta profiles for a portion of station 15 (located within the Gulf Stream), together with the 16-m-smoothed and 0.01 σ_θ-interpolated depth values. This figure provides an idea of the degree of smoothing suffered by the original den-

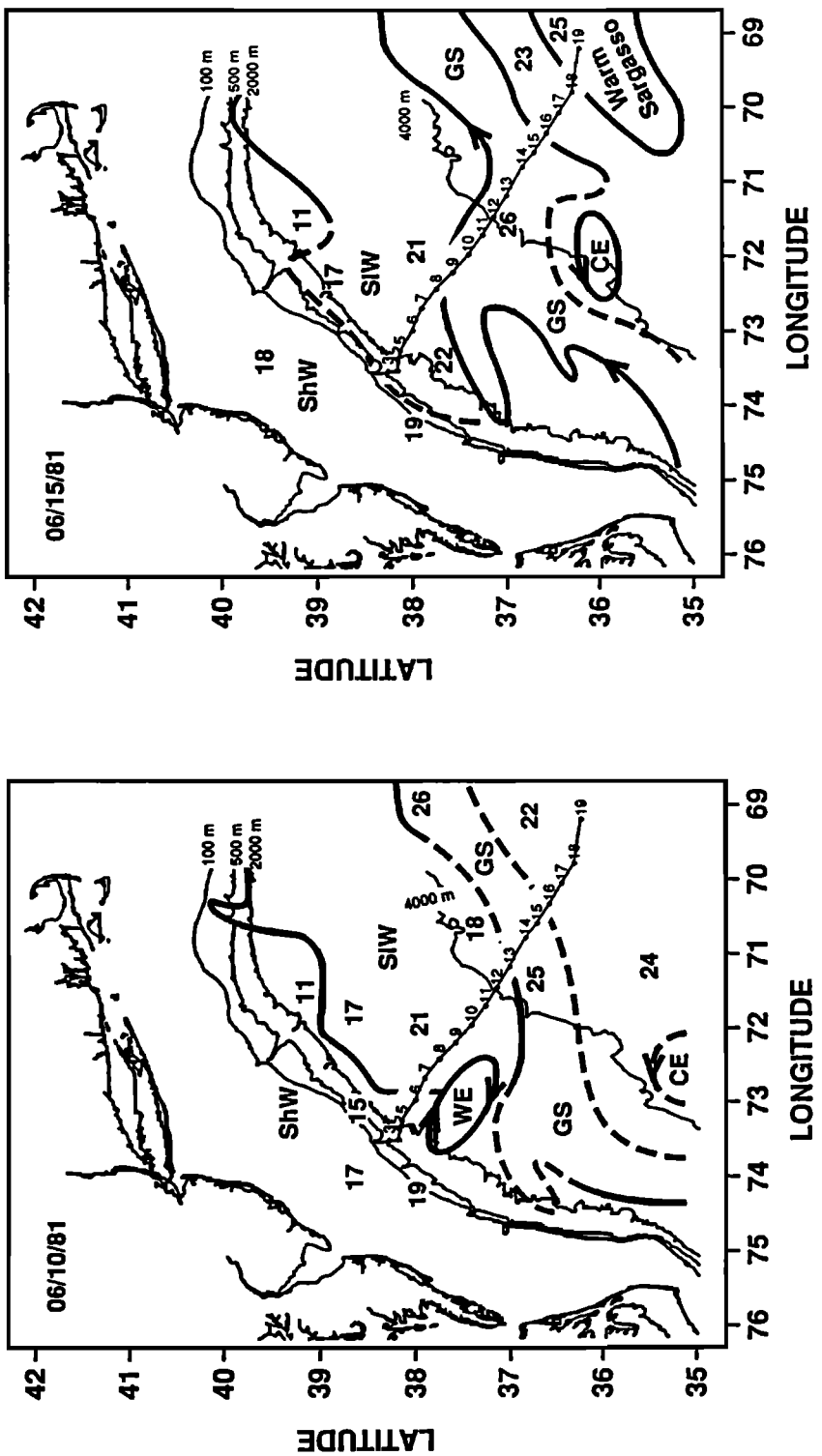

Figure 2. Frontal analysis maps for the region of interest, during June 10 and 15, 1981 (adapted from originals courtesy of Jenifer Clark, NOAA). Also shown is the location of the hydrographic stations used in this study, occupied in the offshore direction between June 12 and 14, 1981.

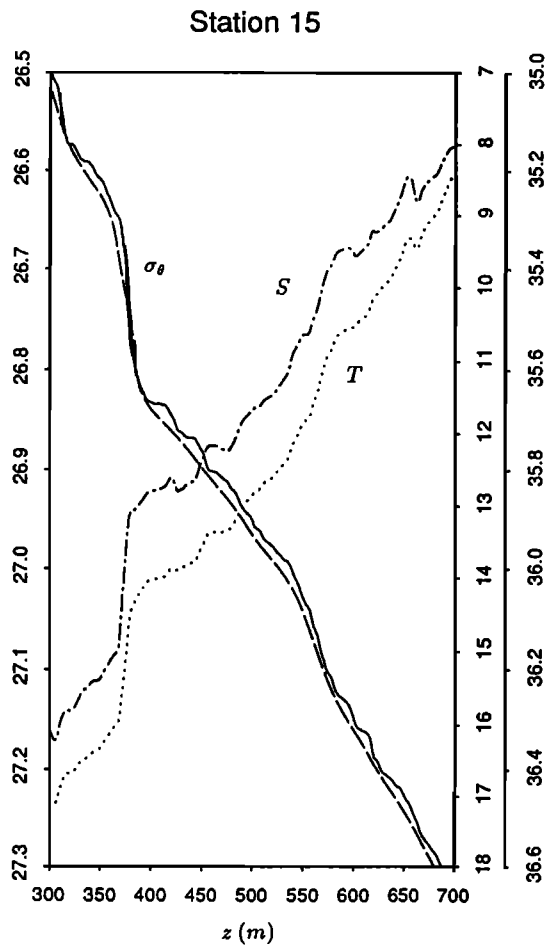

Figure 3. Temperature, salinity and sigma-theta profiles obtained from the unsmoothed data of station 15 in section 36N. Also shown is the smoothed and interpolated density-depth profile (dashed line).

sity data, which eliminates not only all inversions but also removes the small-scale steplike structures. It also shows the relation between salinity, temperature and sigma-theta for a given depth or depth range; these and other aspects will be discussed with detail in section 5.

Figure 4a shows the smoothed σ_θ distribution with the sea surface as the reference pressure, in the Cartesian coordinate system, and Figure 5a presents the derived depth distribution, z, in isopycnic coordinates. The isopycnic coordinates have not been extended above the $26.5\,\sigma_\theta$ surface because near the sea surface the isopycnals are closely packed and the interpolation procedure loses accuracy; the lower limit has been chosen to correspond to the $27.8\,\sigma_\theta$ surface. Hereinafter, except where otherwise noted, our calculations with section 36N will always use the above "smoothed" data (smoothed and interpolated depth field).

4.1. The Jacobian and the Richardson Number

In Figure 5b we present the distribution of j in isopycnic coordinates which, because of the small variations in ρ, closely resembles that of J, and is an index of separation between adjacent isopycnals (hereinafter, according to convention, J and j values shown are absolute values). Several distinct domains are apparent, also recognizable in Figure 4a. The most extensive domain encompasses Sargasso Sea and Gulf Stream thermocline layers, where j is relatively large, about 10^6 m in the upper thermocline and still larger below. Another extensive domain represents the near-surface stratified layers within the Slope Sea and shelf waters, with j values of order 10^5 m. Just underneath this region a band of large j values is seen, about $1 - 3 \times 10^6$ m, representing the residue of the winter pycnostad. Finally, a small but distinct domain, of relatively low j values, below 3×10^5 m, appears in the upper thermocline layers of the Gulf Stream. This is the domain of interest for our present study. Since the corresponding domain is not easy to identify in Figure 4a, we have enlarged it in Figure 4b. In this last figure we have hatched the regions with j less than 3×10^5 m, for $\sigma_\theta > 26.5$; our domain of interest is confined to the hatched areas between stations 13 and 17. In these regions the vertical distance between adjacent isopycnals is relatively small, although this does not stand out in a depth versus distance plot.

As the next step in our analysis, we use (20) to calculate the distribution of the potential ϕ, referenced to the $\sigma_\theta = 27.8$ isopycnal (Figure 6a). The distribution of ϕ resembles those obtained by *Bower et al.* [1985] for three hydrographic sections located some 500 km farther NE (notice, however, that there is a difference of a g factor in these definitions). The along-stream geostrophic velocity in the isopycnic coordinate system is calculated from

$$fv = \frac{\partial \phi}{\partial x}. \tag{34}$$

The velocity field obtained in this manner is shown in Figure 6b. The maximum velocity, referenced to the $\sigma_\theta = 27.8$ isopycnal, is nearly 1 m s^{-1}. We may appreciate that the epipycnal velocity gradient $\partial v/\partial x$ is more intense on the anticyclonic (offshore) side of the stream than on the cyclonic (shoreward) side, contrary to what is usual along level surfaces.

The Ri distribution in section 36N is shown in Figure 7a, with relatively large Ri values (> 40) everywhere except between stations 13 and 17, the position of the Gulf Stream (as usual, throughout this work we always present absolute Ri values). The regions with minima Ri values ($Ri \simeq 3$ - 4) are found in the upper thermocline of the Gulf Stream. The corresponding maximum density eddy diffusivity, as calculated using (12), is 1.3×10^{-5} m^2 s^{-1}. Recall that the Ri values, apparently well above critical, are obtained with the 16-m smoothed and subsequently interpolated values. This was done in order to systematically remove the inversions in the density field, but it also has the effect of reducing the gradients in the highly stratified regions, increasing J and presumably Ri. The results nevertheless show that shear instability is most likely to occur in the upper thermocline, if anywhere.

Note that for (32) to be valid the absolute value of j cannot be too small. Some physical process is likely to set a limitation on the squeezing together of the isopy-

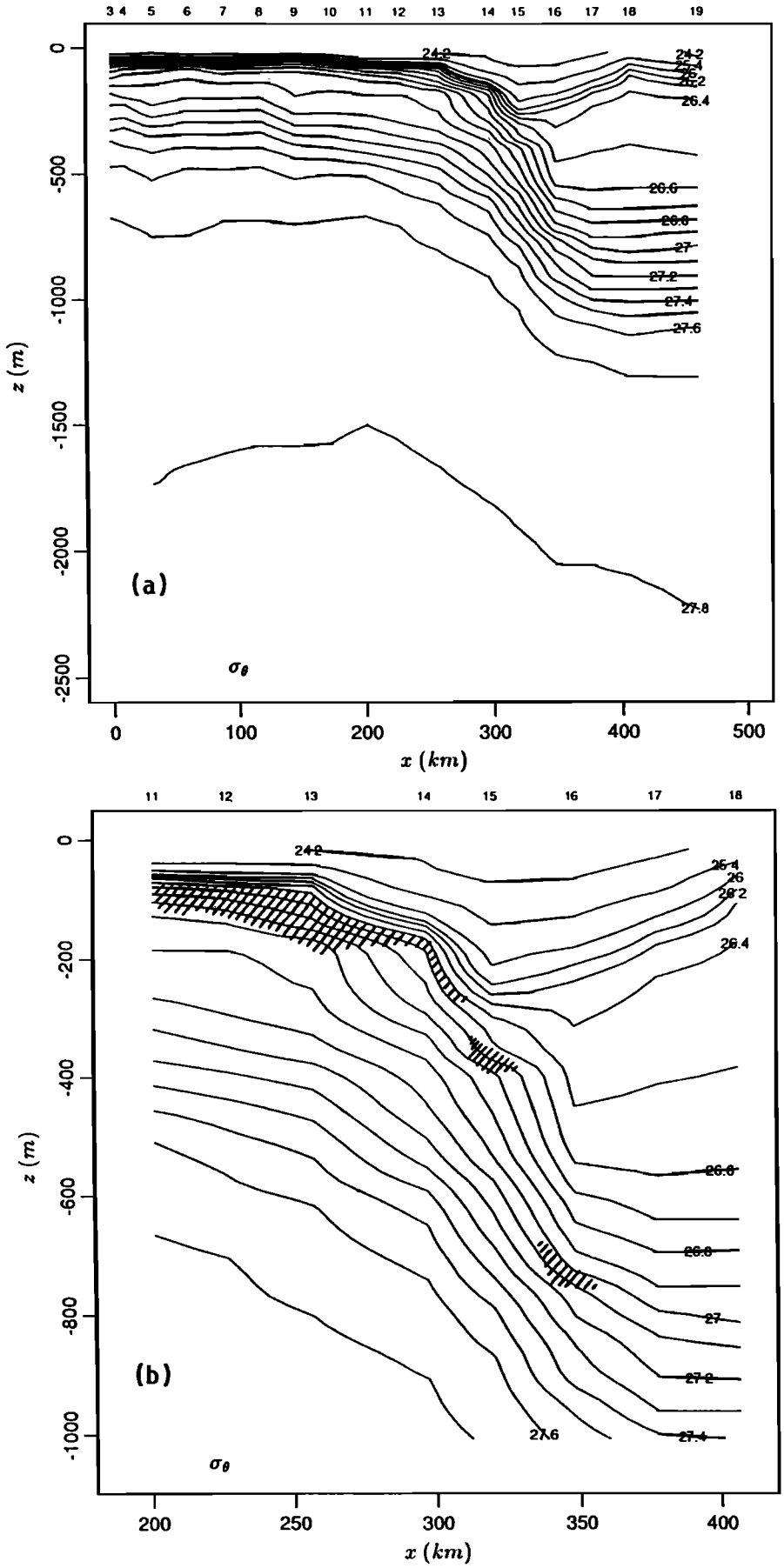

Figure 4. (a) Smoothed (16-m-averaged) sigma-theta, σ_θ, in Cartesian coordinates. (b) A close-up for the top 1000 m of the Gulf Stream. For $\sigma_\theta > 26.5$, the areas corresponding to $j < 3 \times 10^5$ m have been hatched.

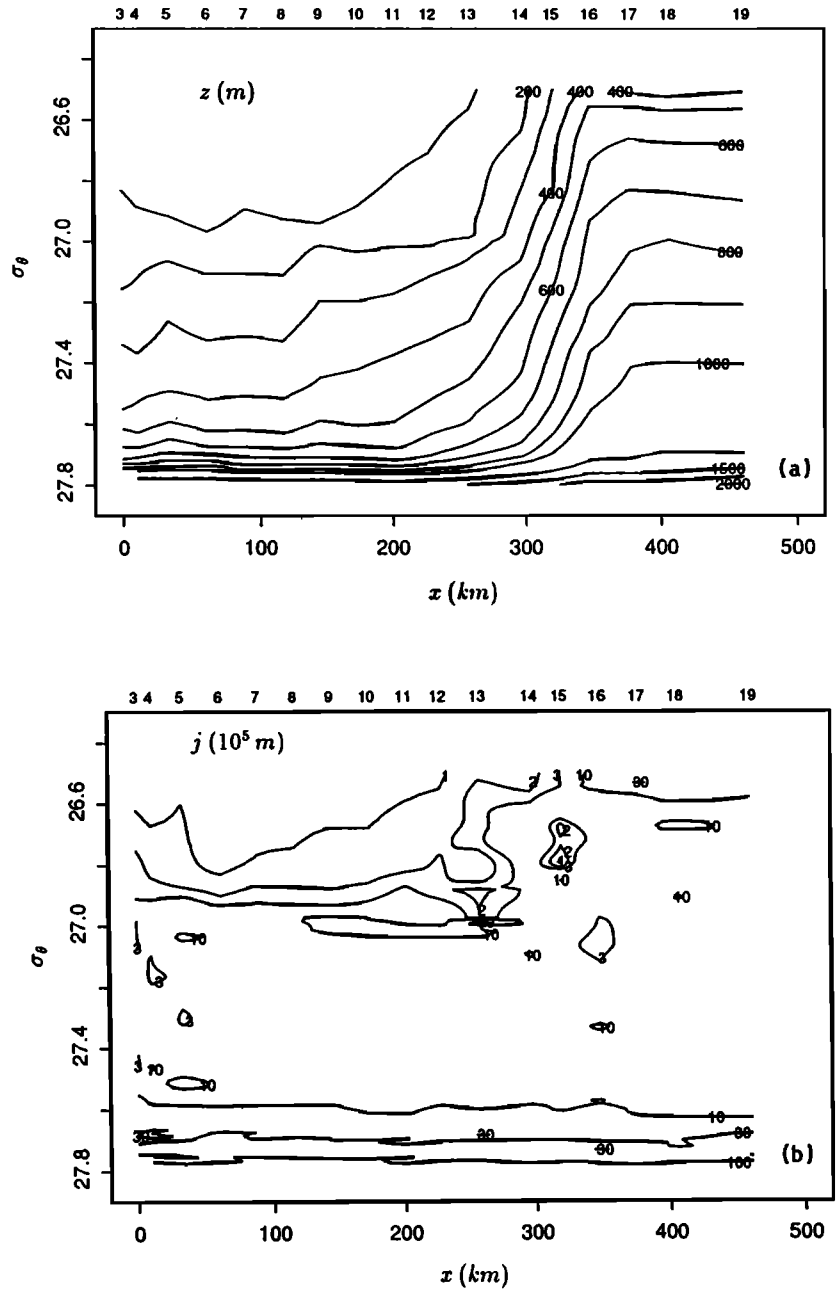

Figure 5. (a) Smoothed and interpolated depth, z. (b) Separation index, $j = \rho J$.

cnals, the reduction of j. The appearance of relatively small Ri numbers (Figure 7a) within the domain of small j, supports the idea that the limitation is due to hydrodynamic instability and mixing once two isopycnal surfaces get too close. As discussed after (11), this is due to shear enhancement developing with increased stratification if $\partial v/\partial \rho$ remains constant or increases. This antisimilar character of the j and $(\partial v/\partial \rho)^2$ distributions may be seen by comparing Figures 5b and 7b.

The appearance of mixed regions and inversions in the potential density field, although disturbing to the isopycnic formulation, is a necessary part of the instability and mixing processes to which we have referred. It is unavoidable that any mixing reduces stratification (increases J), and creates well-mixed regions and local inversions in time and space if Kelvin-Helmholtz instabilities and billows are responsible for this process [*Thorpe*, 1973, 1987]. Smoothing and interpolation of the data considerably modifies the local z values, the large extent of this change being related to the similar vertical sizes of the well-mixed regions ($\sim$ 20 m) and the smoothing interval (16 m). The substantial effect of smoothing on these regions may be appreciated in Figure 3, where both unsmoothed and smoothed density profiles are shown for station 15.

The observed minimum smoothed Ri values suggest the existence of locally much smaller, near critical Ri. Equations (20) and (34) yield the thermal wind equation in isopycnic coordinates:

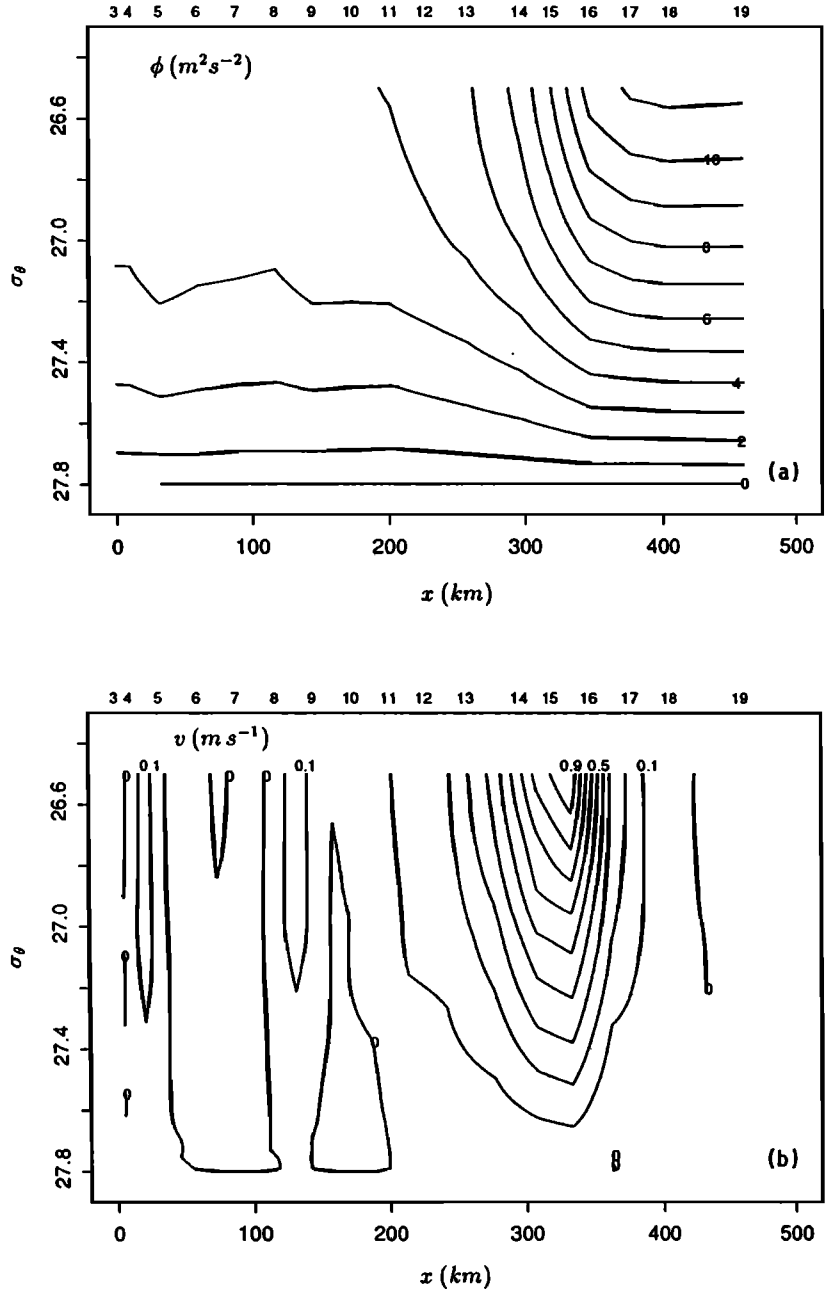

Figure 6. (a) Montgomery potential, ϕ, referred to the $27.8\,\sigma_\theta$ surface. (b) Along-stream geostrophic velocity, v, referred to the $27.8\,\sigma_\theta$ surface.

$$f\frac{\partial v}{\partial \rho} = \frac{g}{\rho}\frac{\partial z}{\partial x}. \tag{35}$$

Substitution in (11) then approximates Ri in isopycnic coordinates by

$$Ri = \left(\frac{f^2\rho}{g}\right)\frac{J}{\left(\frac{\partial z}{\partial x}\right)^2}. \tag{36}$$

Equation (36) shows that Ri depends directly on J and inversely on the square of the horizontal depth gradient. Vertically averaging smoothes the density field, and subsequent interpolation to sigma-theta surfaces produces a smoothed depth field and reduces the minima in J. Figure 8 shows the 2-m-averaged original (which we call "unsmoothed") j distribution in vertical coordinates, for the region of the Gulf Stream. In this figure we present contour lines only for 10^0 and 10^3 units (10^5 and 10^8 m), which correspond to well-stratified and well-mixed regions, respectively. The large variability of this field reflects mainly the existence of numerous well-mixed thin layers (of about 10 - 20 m). The effect of smoothing in reducing this variability is clear if we compare this figure with Figure 5b, where we presented the j field obtained from the smoothed data (in isopycnic coordinates).

The smoothing problem is indeed a difficult one. A careful study on data smoothing and its effect on Ri

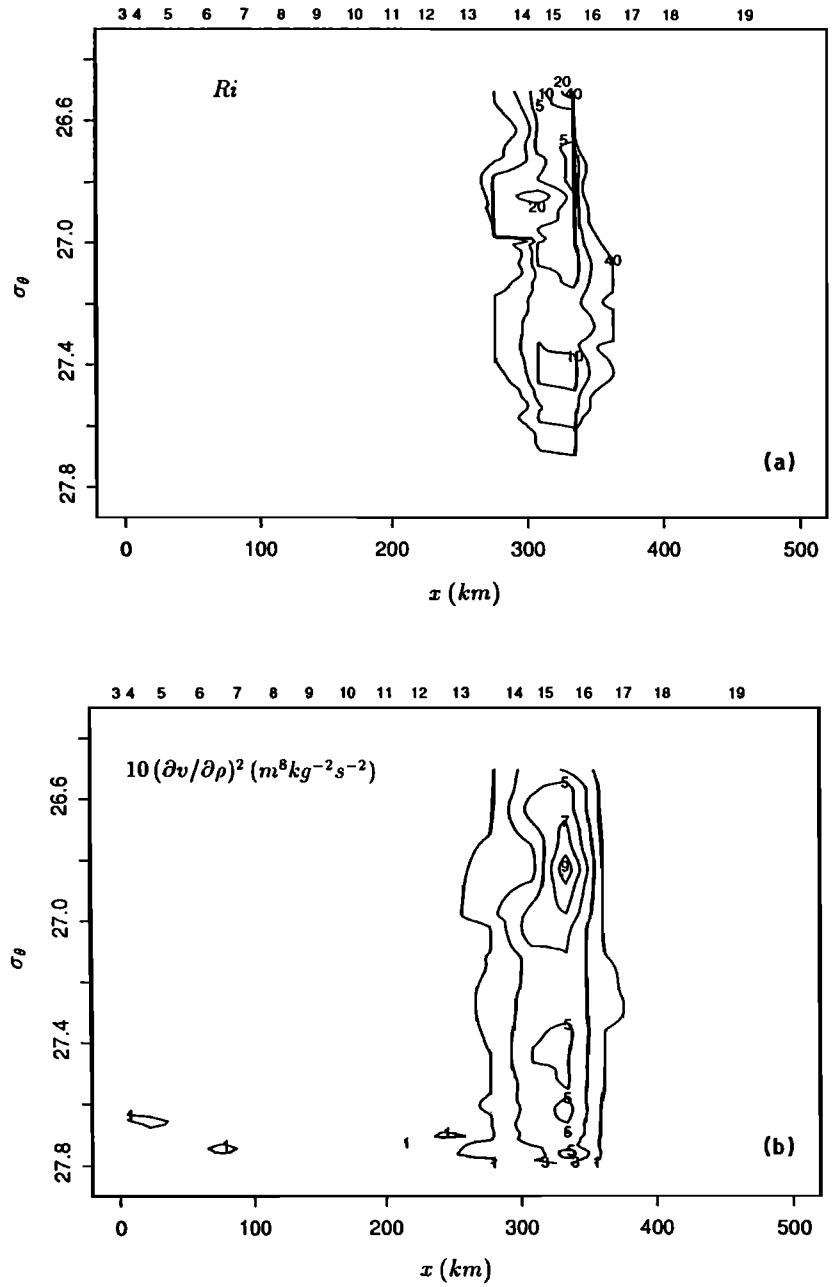

Figure 7. (a) Richardson number, Ri. (b) Square of the diapycnal shear, $(\partial v/\partial \rho)^2$.

is due to *Miller and Evans* [1985]. Our main concern here is to do as little smoothing as possible in order to retain the mixing signature. We recognize that there may be shear mixing induced by ageostrophic motions, which cannot be evaluated from the density field. There are two things, however, to keep in mind. First, that the values calculated for $\partial v/\partial \rho$ (from $\partial z/\partial x$) closely give the geostrophic contribution: for stations separated many kilometers within the Gulf Stream, the slopes obtained from one single realization of the density field will be very similar to those calculated from the long-time "mean" density field. And second, that Ri will decrease with decreasing J (increasing stratification) if $\partial v/\partial \rho$ does not decrease. In these circumstances, instabilities due to ageostrophic motions would decrease J while $\partial v/\partial \rho$ is nearly unchanged. We may conclude hence that our calculations for Ri are an overestimated index of dynamic stability.

4.2. Vorticity and Potential Vorticity

Figure 9a presents the distribution of the absolute vorticity, $\zeta + f$, in isopycnic coordinates. The vertical component of the relative vorticity has been approximated by $\zeta = \partial v/\partial x$, where v is the along-stream geostrophic velocity. The planetary vorticity at this location is about 8.7×10^{-5} s^{-1}. The figure reveals the cyclonic and anticyclonic sides of the Gulf Stream, with absolute vorticity larger (up to about 10×10^{-5} s^{-1}) and smaller (down to nearly 6×10^{-5} s^{-1}) than

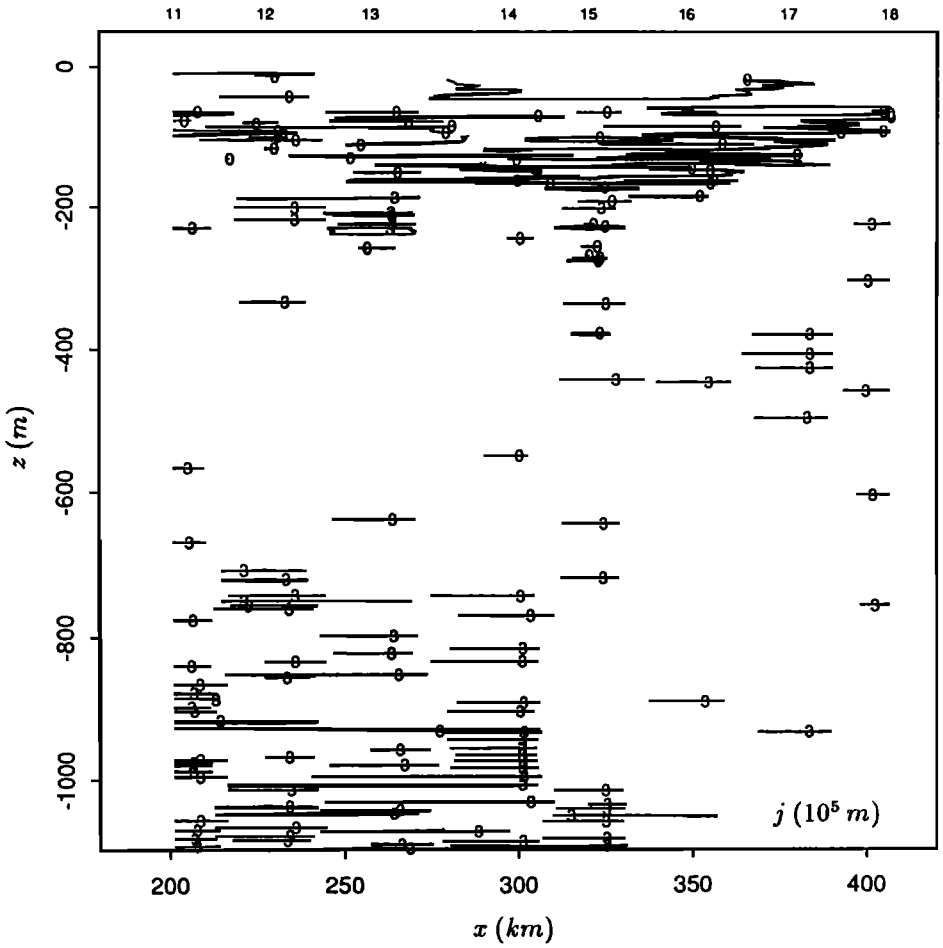

Figure 8. Separation index, $j = \rho J$, in Cartesian coordinates, from the unsmoothed density field (the region shown is the same as in Figure 4b). Zero stands for 10^0 units (10^5 m), and 3 for 10^3 units (10^8 m).

the planetary vorticity. We may also appreciate that in the upper thermocline layers ($26.5 < \sigma_\theta < 27.2$), the peak relative vorticity ζ is about twice larger on the cyclonic than on the anticyclonic side. However, the relative changes of absolute vorticity are clearly much smaller than those of the Jacobian, roughly one-third versus a factor of 5.

Figure 9b presents the distribution of the isopycnic potential vorticity q, as defined by (29) (again, hereinafter q values shown have dropped the negative sign). This is similar to the distribution of the Jacobian and shows the same domains as described above. In particular, within the Gulf Stream the potential vorticity attains relatively large values, above 3.5×10^{-10} m^{-1} s^{-1}, versus 10^{-10} m^{-1} s^{-1} for the surrounding waters. The range of variation is thus about a factor of 3 to 5, slightly less than the range of the Jacobian.

The figures establish the existence of an anomalous region of relatively small j and large q, with extreme values in the core of the Gulf Stream ($26.65 < \sigma_\theta < 26.8$). It is worthy to point out that this intense q anomaly may also be seen in the results of *Roemmich and Wunsch* [1985], obtained using the same data set. They presented the potential vorticity on the $\sigma_\theta = 26.75$ isopycnal (their Figure 15b, not reproduced here), for the whole transatlantic section approximately along 36° N, of which ours is the western portion. The magnitude of this anomaly ($\simeq 6 \times 10^{-10}$ m^{-1} s^{-1}) is in good agreement with our estimates and shows to be about 5 times larger than the background level in the interior of the subtropical gyre ($\simeq 1 - 1.5 \times 10^{-10}$ m^{-1} s^{-1}). The narrow confines of the anomaly are such that it quickly becomes imperceptible in any spatially smoothed map (e.g., Figure 14b by *Roemmich and Wunsch* [1985]).

As discussed above (equations (21) to (32)), diapycnal convergence or divergence may be directly related to the material changes of j and q whenever the other contributions are considerably smaller. The fact that the anomalies are present in both the j and q fields, but not in the absolute vorticity field, suggests that this is indeed the case (equation (33)). However, at this point we cannot tell whether the diapycnal convergence is producing or removing the observed anomalies. We argue below that it is the inertial, nearly inviscid, evolution of Gulf Stream meanders that causes instability (and low Ri numbers), which then leads to diapycnal convergence and mixing.

Also relevant to this discussion are the potential vor-

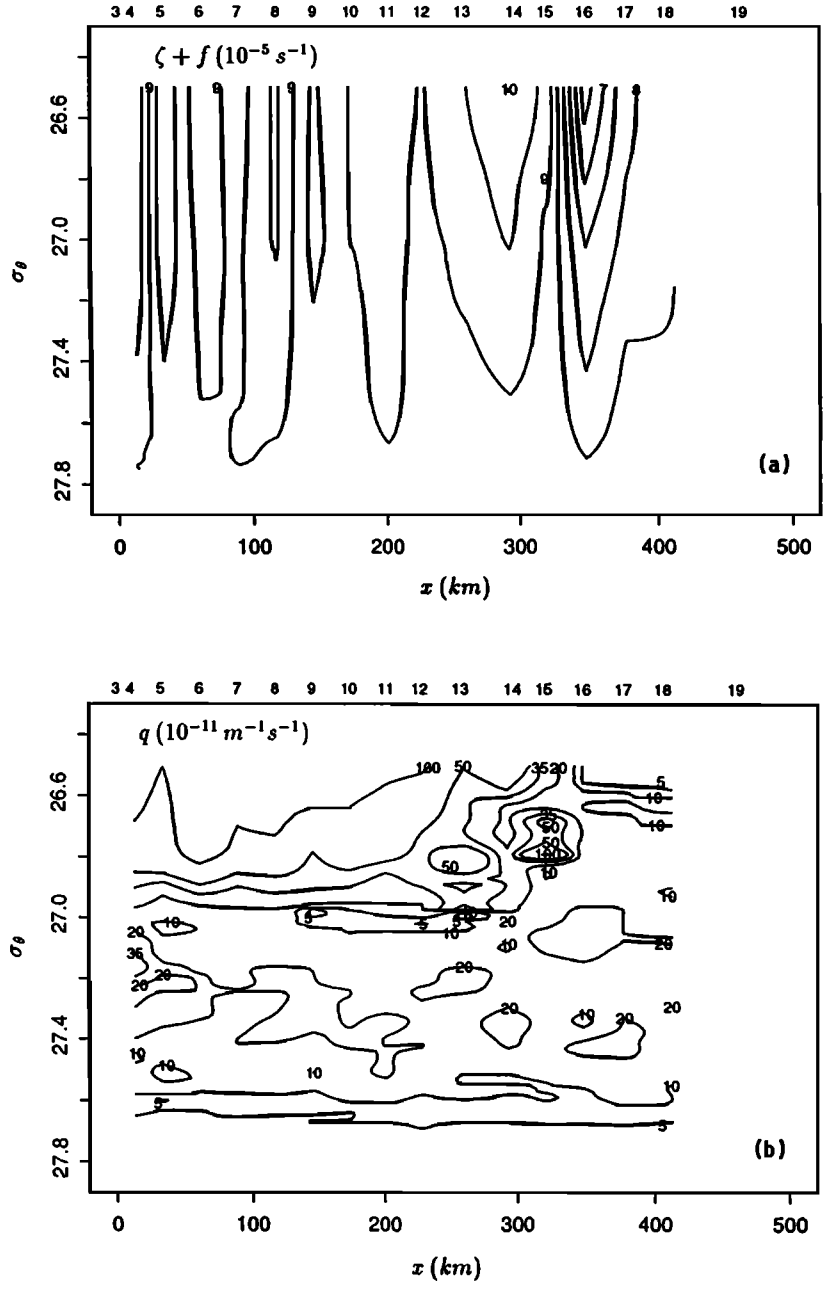

Figure 9. (a) Absolute vorticity, $\zeta + f$. Planetary vorticity at this location is about 8.7×10^{-5} s^{-1}. (b) Potential vorticity, q.

ticity distributions calculated by *Bower et al.* [1985] and *Leaman et al.* [1989]. *Bower et al.* [1985] showed these for several Gulf Stream sections. In all their sections (their Figures 1 to 4, not reproduced here), patches of anomalously large potential vorticity are clear within the upper thermocline of the Gulf Stream. *Leaman et al.*'s [1989] sections do not show such anomalies, presumably because they are not individual surveys but were calculated by averaging an ensemble of a large number of surveys at the same location.

4.3. Diapycnal Convergence

Equation (13) provides the basis for estimating w_ρ from the J and Ri distributions previously calculated. From w_ρ we can also determine w_d and $\partial w_\rho/\partial\rho$. For generality, and since the exact value of K_0 is unknown, these quantities are expressed in terms of K_0. We give the results as multiples of K_0, as well as actual values with our best choice of K_0 (2.6×10^{-3} m^2 s^{-1}). For simplicity we omit the units of the former but we give the units for the latter.

Figure 10 shows a few contours of the distribution of w_ρ in section 36N. Solid and dashed lines refer to positive and negative values, respectively. In this figure we have labeled only the contours with $(\pm)\,10^{-7}K_0$ [2.6×10^{-10} kg m^{-3} s^{-1} $\simeq 2.6 \times 10^{-10}\sigma_\theta$ s^{-1}]. Additional contours changing by $(\pm)\,2 \times 10^{-7}K_0$ [5.2×10^{-10} kg m^{-3} s^{-1} $\simeq 5.2 \times 10^{-10}\sigma_\theta$ s^{-1}] are also shown, but

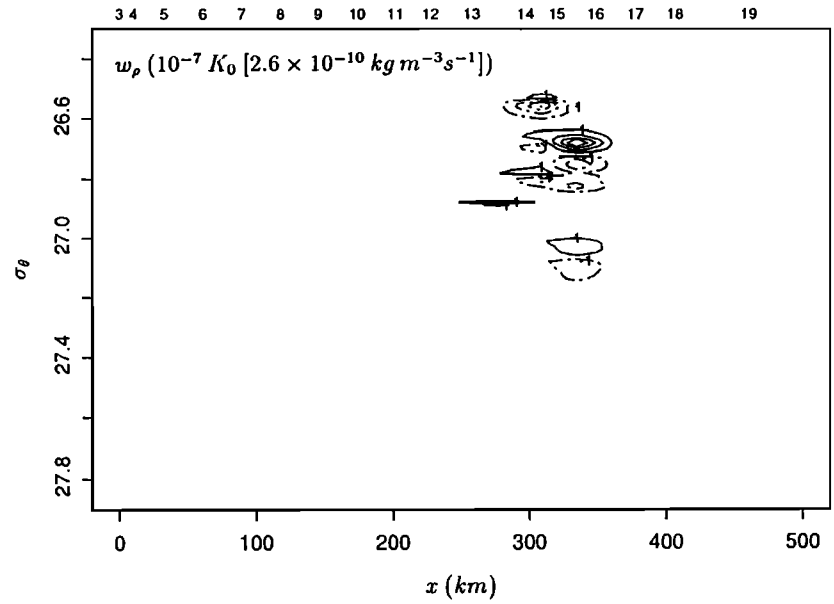

Figure 10. Density tendency, w_ρ. Solid and dashed lines refer to positive and negative values, respectively. Only the contours with $(\pm)\, 10^{-7} K_0$ [2.6×10^{-10} kg m^{-3} s^{-1} $\simeq 2.6 \times 10^{-10}\, \sigma_\theta$ s^{-1}] are labeled. Additional contours, changing by $(\pm)\, 2 \times 10^{-7} K_0$ [5.2×10^{-10} kg m^{-3} s^{-1} $\simeq 5.2 \times 10^{-10}\, \sigma_\theta$ s^{-1}], are shown.

they have not been labeled in order to avoid overlapping numbers. The main purpose of the figure is to show the total absence of significant values except in the upper thermocline of the Gulf Stream. Similar results hold for w_d and $\partial w_\rho / \partial \rho$, not shown here.

In Figures 11 to 13 we present the results for the region where mixing takes place. Figure 11 contours separately the two contributions to w_ρ in (13), while Figure 12a shows the combined result. The first contribution to w_ρ (first term on the right-hand side of (7) or (13)) depends on the diapycnal gradient of Ri; we denote this contribution by the superscript r, w_ρ^r (Figure 11a). The second contribution depends on the diapycnal gradient of J; it is denoted with the superscript j, w_ρ^j (Figure 11b). Contour intervals are in units of $10^{-7} K_0$ [about $2.6 \times 10^{-10}\, \sigma_\theta$ s^{-1}]. Solid and dashed lines refer to positive and negative values, respectively.

A striking feature in these figures is their patchy character. A patch of positive values usually alternates with a patch of negative values, of similar size, both of about the same magnitude. The diapycnal extension of the patches varies but does not exceed about $0.05\, \sigma_\theta$. Within the Gulf Stream the directions of w_ρ^r and w_ρ^j agree everywhere. The maximum contribution from the term depending on the Ri variation is roughly twice that from the term depending on the J variation.

Figures 12b and 13a present the corresponding w_d and $\partial w_\rho / \partial \rho$ distributions for the same enhanced region. In these figures the contours are labeled in units of $10^{-4} K_0$ [2.6×10^{-7} m s^{-1}] and $10^{-5} K_0$ [2.6×10^{-8} s^{-1}], respectively. Solid and dashed lines refer to positive and negative values. Again, the patchy nature of the fields is evident. With our best estimate, $K_0 = 2.6 \times 10^{-3}$ m^2 s^{-1}, we find absolute maximum values for w_ρ, w_d and $\partial w_\rho / \partial \rho$, of about $2.6 \times 10^{-9}\, \sigma_\theta$ s^{-1}, 6.6×10^{-7} m s^{-1}, and 1.1×10^{-7} s^{-1}, respectively. By comparing these estimates with the maximum possible contributions to w_ρ (w_d) due to nonlinearities in the equation of state (section 2.2), we ratify their omission.

Recall that w_d is the actual diapycnal velocity, not an epipycnal contribution to the total vertical velocity. The above values are certainly much smaller than those we had obtained in PC, by about 2 orders of magnitude, but this is likely the result of smoothing. We showed earlier that smoothing the depth field, z (in isopycnic coordinates), has a large effect on the Jacobian, and hence on the Richardson number. Equation (13) shows that smoothing also must have a large effect on the diapycnal velocity. This is clear if we realize that this expression not only includes a high power of J (and Ri), but it also includes $\partial J / \partial \rho$ (and $\partial Ri / \partial \rho$). Figure 8 indeed shows that the unsmoothed J values can change very rapidly in the diapycnal direction.

We may now compare the $\partial w_\rho / \partial \rho$ field with the distribution of j and q. In view of (22), if the calculated $\partial w_\rho / \partial \rho$ field is the result of the observed j distribution, then any strong signal in $\partial w_\rho / \partial \rho$ must be related to an anomaly in the j distribution. In Figure 13b we present an enhancement of the j field for the Gulf Stream region, with the same spatial scaling as in the previous figures. A comparison of this figure with Figure 13a shows that the location of negative maxima of $\partial w_\rho / \partial \rho$ (between stations 14 and 16, centered at about $\sigma_\theta = 26.7$ and 26.8; also near $\sigma_\theta = 26.55$ at station 14), correspond to minima in j. This supports the hypothesis that large diapycnal convergence is associated with the

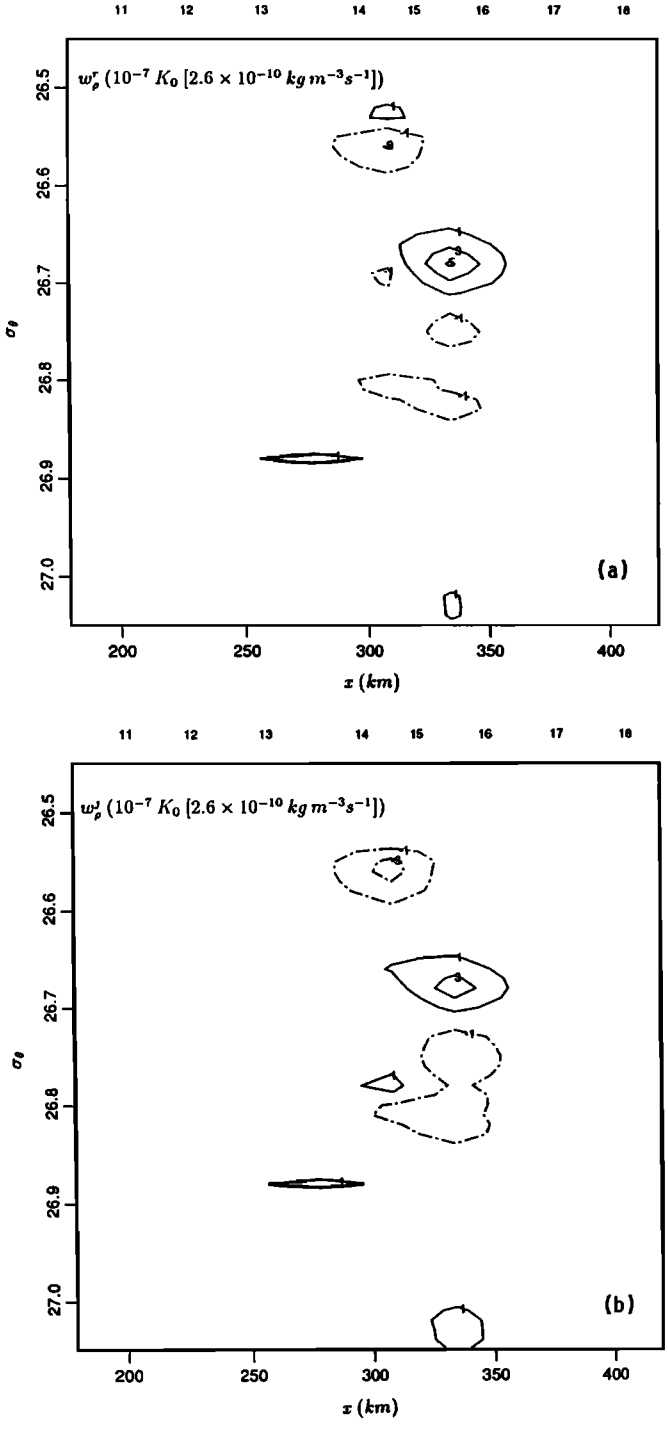

Figure 11. Contributions to the density tendency (equation (12)) (a) w_ρ^r and (b) w_ρ^j. Solid and dashed lines refer to positive and negative values, respectively.

tightly packed isopycnals. Similar agreement exists for the q field (see Figure 9b; its enhancement is not shown here).

5. Frontogenesis and Mixing

It is reasonable to suppose that large diapycnal velocities are the manifestation of intermittent mixing events, triggered by subcritical Ri values, associated with increased horizontal depth gradients ($\partial z/\partial x$) and increased vertical density gradients ($\partial \rho/\partial z$). The generation of such strong gradients, or frontogenesis, has long been known to occur in atmospheric jet stream waves [*Newton*, 1954, 1978; *Staley*, 1960; *Palmén and Newton*, 1969]. In the jet stream the density gradients are increased between a crest and the subsequent trough, while they decrease after the trough. Similarly, we may anticipate that the separation between adjacent isopycnal layers is likely to be reduced during analogous phases of Gulf Stream meanders. Our case study corresponds precisely to the passage of such a meander's phase (Figure 2).

The mechanism for frontogenesis in the Gulf Stream still needs to be established. One possibility is a time-dependent deformation horizontal velocity field associated to the passage of the meanders. This field should be vertically sheared, capable not only of horizontal compression but also of differential tilting of the isopycnals. During the shrinking of the isopycnal layers, or frontogenetical stage, the horizontal depth gradient would increase and the Jacobian would decrease (and the potential vorticity increase, corresponding to the "dynamic frontogenesis" discussed by *Bleck et al.* [1988]). During this stage the diapycnal shear should also increase (through the thermal-wind relation) and create subcritical Ri regions. This hypothesis is consistent with the observations by *Bane et al.* [1981], in the Gulf Stream off the South-Atlantic Bight, that the intensification of the horizontal velocity in meanders is accompanied by an increase of the vertical velocity gradient, $\partial v/\partial z$. It is also consistent with *Kunze et al.* [1990] observations in the thermocline off southern California, where low Richardson numbers were achieved by an increase in $\partial v/\partial z$ rather than by a decrease in $\partial \rho/\partial z$.

Figure 3 shows the original (unsmoothed) 2-m-averaged temperature, salinity and density data for station 15, which cuts across the Gulf Stream. Two types of regions are clear: a highly stratified one centered at $\sigma_\theta = 26.73$ and several others with a staircaselike density distribution. The staircase is best defined in the $26.8 < \sigma_\theta < 27.0$ and $27.1 < \sigma_\theta < 27.2$ ranges, also clear near $\sigma_\theta \simeq 26.60$. Figure 3 also shows the smoothed and interpolated density-depth profile. The highly stratified region is still apparent in this smoothed representation, but the well-mixed layers disappear (see also Figures 5b and 8 for the separation index j). This is because the interpolation to σ_θ surfaces cannot show well-mixed regions.

The steplike density structure in the upper thermocline resembles those commonly attributed to double-diffusive intrusions (for reviews see *Turner* [1973] and *Garrett* [1982]). *Gregg and Sanford* [1980] reported several meters thick temperature stepped structures in the upper thermocline of the Gulf Stream and interpreted them to be predominantly caused by salt-fingering. Their 50-m-averaged Richardson numbers were supercritical, but this may have been caused by vertical averaging, as discussed earlier. Other studies, indeed, have held intermittent turbulent shear mixing

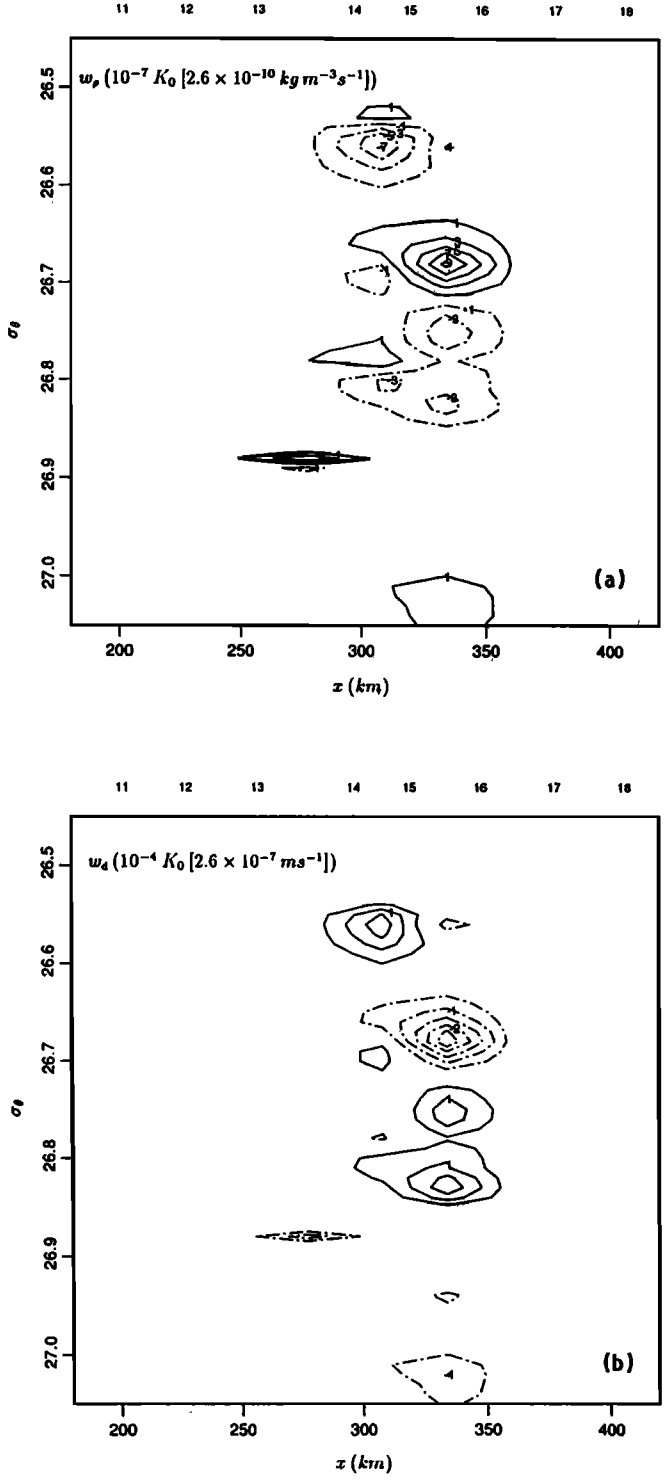

Figure 12. (a) Density tendency, w_ρ and (b) diapycnal velocity, w_d. Solid and dashed lines refer to positive and negative values, respectively.

responsible for staircase structures [*Kullenberg et al.*, 1974; *Gregg et al.*, 1986; *Marmorino*, 1987; *Toole and Schmitt*, 1987]. *Gregg et al.* [1986] reported steplike density structures in a diffusively stable thermocline, which they ascribed to the breaking of near-inertial internal waves. They found dissipation to vary in the vertical, with alternating high and low values in adjacent layers. Their results suggest that the start and the end of a burst of high dissipation may be associated with 10-m-averaged subcritical Richardson numbers (their Figures 9a and 11, not reproduced here). *Kundu and Beardsley* [1991], analyzing upwelling on the west coast of the United States, found near-critical Ri numbers in the upwelled main thermocline associated with high vertical mean shear. They speculated on the existence of

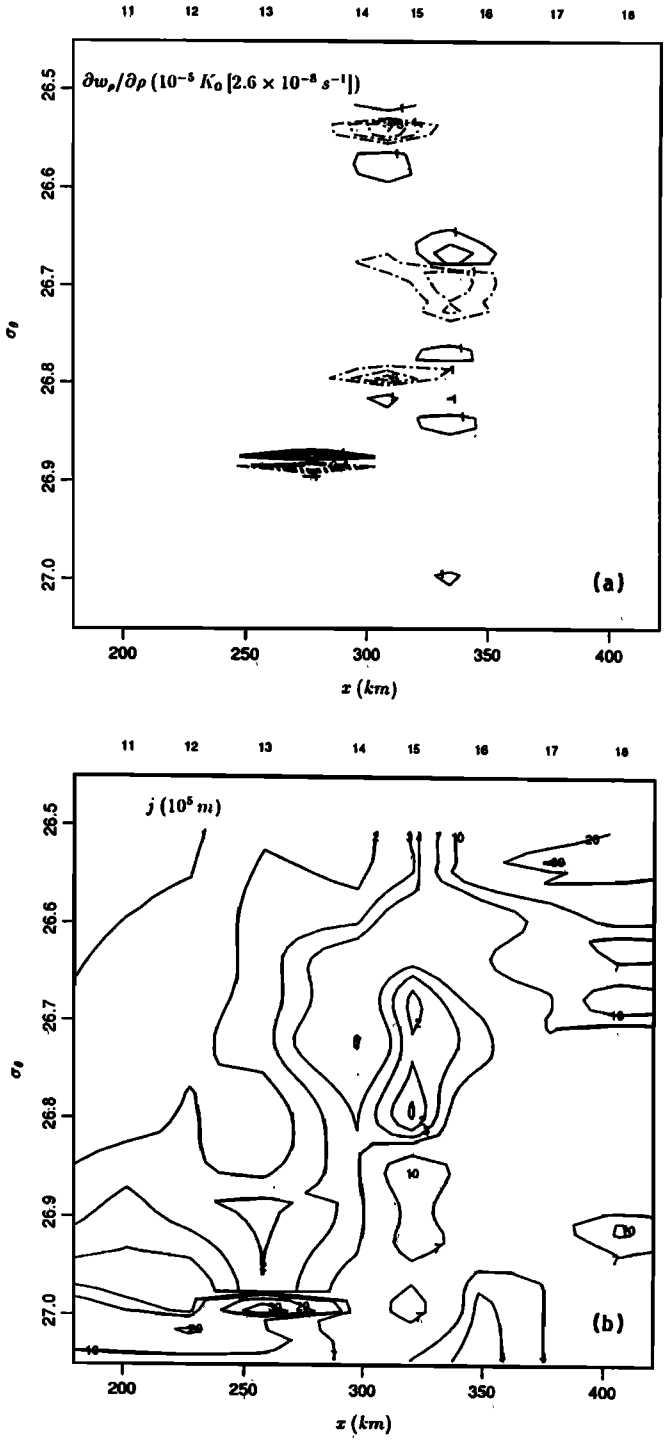

Figure 13. (a) Diapycnal divergence, $\partial w_\rho/\partial\rho$. Solid and dashed lines refer to positive (divergence) and negative (convergence) values, respectively. (b) Separation index, $j = J\rho$.

thin interface layers with subcritical Ri numbers, while mean measured values were above critical. Critically stable regions have been reported in the equatorial undercurrent by *Chereskin et al.* [1986], *Toole et al.* [1987] and *Peters et al.* [1988], and in the main oceanic thermocline by *Eriksen* [1978]. *Eriksen* [1987] also reported Ri values in the seasonal thermocline to be frequently subcritical, at times when diapycnal mixing appeared to be intense.

In Figure 14 we show the enhancement of two regions of the original data for station 15. Figure 14a presents the highly stratified region of thickness $0.18\sigma_\theta$, centered at $\sigma_\theta = 26.73$, which is responsible for anomalously small Jacobians. Figure 14b shows the steplike structure immediately below it, on a density scale about 3 times larger. The density thickness of the small j regions ("risers" in the staircase) is variable, typically of 0.02 - 0.04 σ_θ. The vertical thickness of these stratified regions is about 20 m, roughly the same as reported for similar structures in the thermocline [*Toole and Schmitt*, 1987; *Marmorino*, 1987; *Itsweire et al.*, 1989]. Adjacent to the minima in j we find well-mixed regions ("treads" in the staircase). Their length scale is also of about 20 m. We may appreciate that the well-mixed layer immediately below the highly stratified region is not characterized by temperature and salinity inversions, and it could be the result of vertical overturning activity. Farther below appear temperature and salinity inversions which are not accompanied by density inversions and cannot be produced by local vertical mixing. These inversions are probably produced by lateral advection, associated with thermohaline intrusions as discussed, for example, by *Gregg and Sanford* [1980]. A third mechanism, double-diffusive mixing, may be responsible for some of the steps of small vertical size.

Instability and mixing in the upper thermocline layers was first suggested by the epipycnal nutrient distribution (PC) and later confirmed by the dynamic anomalies and diapycnal velocities obtained from the smoothed depth field. Further evidence is given by the isopycnic distribution of $\overline{w'\rho'} = K/J$, w_ρ and $\partial w_\rho/\partial\rho$ between stations 15 and 16 of section 36N, where the latter quantities are calculated using (13) (Figure 15). In general, the maxima in the vertical Reynolds density flux are associated with the packing of the isopycnals, the largest value centered at $\sigma_\theta = 26.73$, the location of the minimum of j in Figures 5b and 13b (the minimum of Ri in Figure 7a).

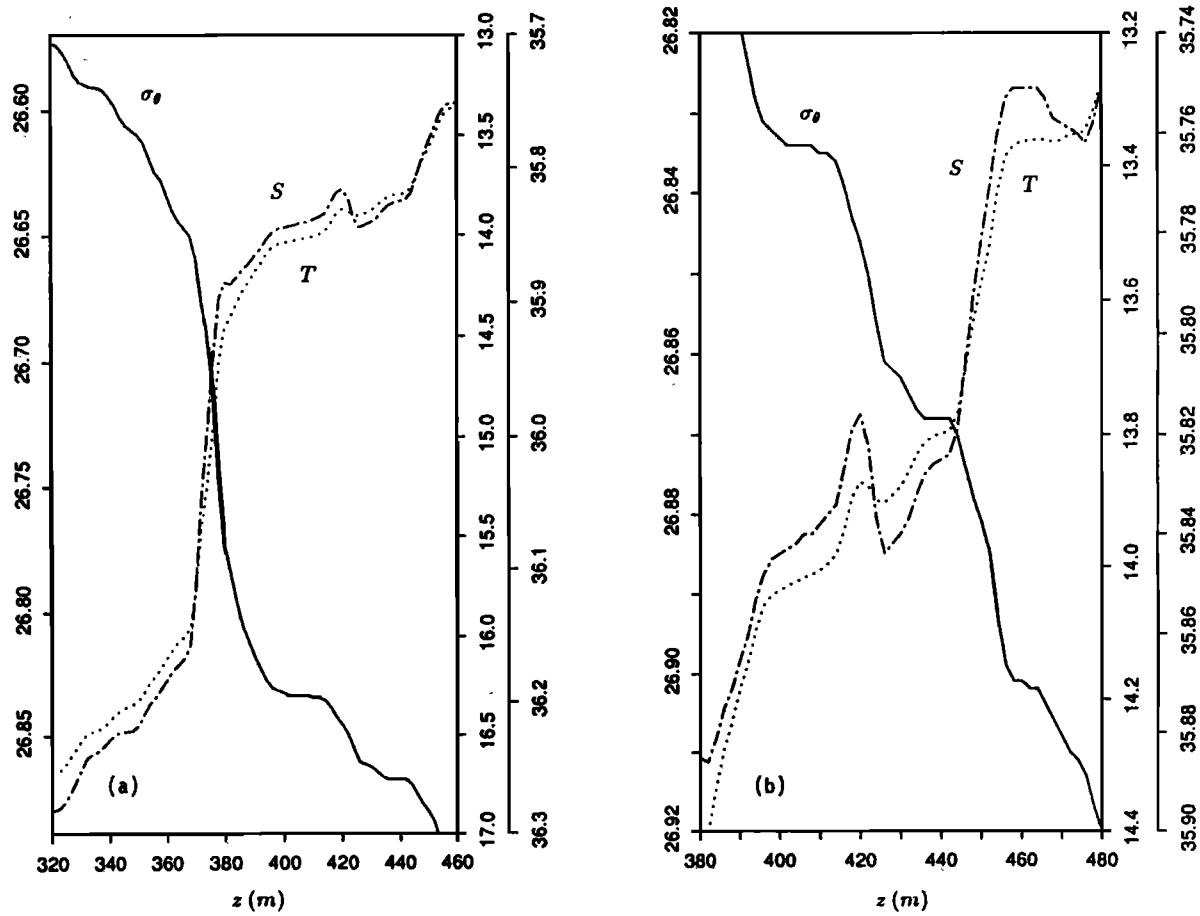

Figure 14. Details of the temperature, salinity and sigma-theta profiles, using the unsmoothed data of station 15 (see Figure 3). (a) A highly stratified region centered at $\sigma_\theta = 26.73$ and (b) the underlying steplike structure.

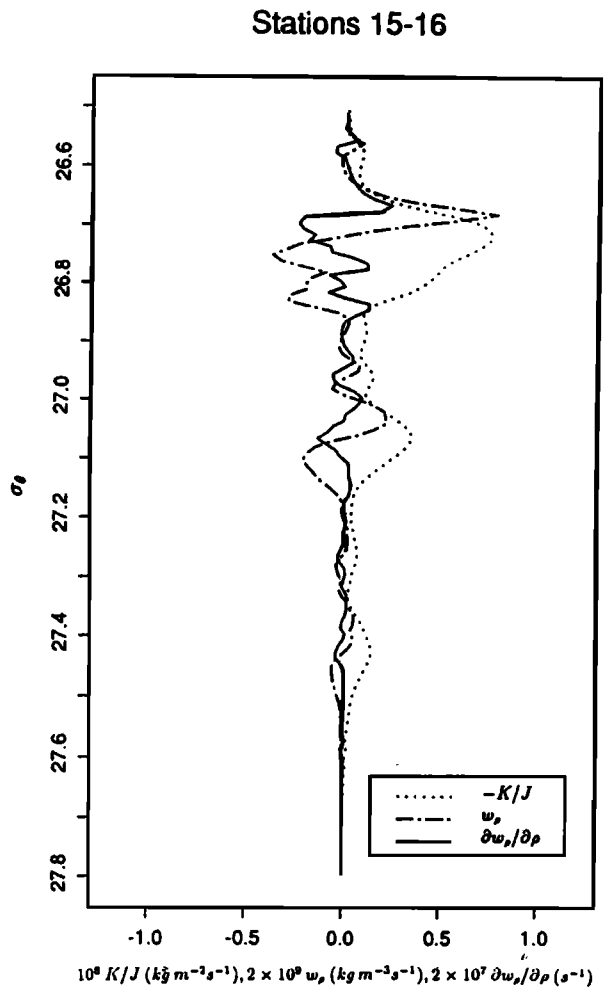

Figure 15. Vertical Reynolds density flux, density tendency, and its diapycnal gradient, as calculated from the smoothed data of stations 15 and 16. The dotted line is the calculated $\overline{w'\rho'} = K/J$ distribution, and the dashed and solid lines the corresponding w_ρ and $\partial w_\rho/\partial\rho$ profiles.

In order to explain some of the observed features in the distribution of the diapycnal velocity, we have constructed a simple model of the vertical Reynolds density flux, $F_z = \overline{w'\rho'}$, within the upper thermocline layers of the Gulf Stream. This model is essentially equivalent to *Phillips* [1972] mechanism of instability in stratified shear flow [see *Posmentier*, 1977; *Ruddick et al.*, 1989]. *Phillips* [1972] justified that, if the turbulent density diffusivity decreases fast enough with the Richardson number, then perturbations in the density gradient will grow leading to the formation of a steplike structure. We wish to center our model, however, on the analysis of the effects caused by localized subcritical Ri numbers due to small Jacobians and large diapycnal shear, i.e., the second equality in (11). This equality, together with a relation of the Munk-Anderson type, states that Ri and K will decrease in response to an increase of the vertical density gradients (the basis of Phillips mechanism) only if the diapycnal shear remains constant or increases. Additionally, our model will allow us to obtain rough estimates for the intensity of the unsmoothed diapycnal velocity field.

We start by asuming that the vertical Reynolds density flux distribution develops a maximum on some isopycnal of the upper thermocline, say $\sigma_m = 26.73$. We idealize this by a hyperbolic secant distribution:

$$\overline{w'\rho'} = \delta\, sech\left[\frac{(\sigma_\theta - \sigma_m)}{\beta_1}\right], \qquad (37)$$

where $\delta \equiv \overline{w'\rho'}_{max}$, and β_1 is the scale, in σ_θ units, of the mixing region.

The vertical Reynolds density flux can be related to the Jacobian with the help of (6), (12) and (11),

$$\overline{w'\rho'} = \frac{K_0(1+10Ri)^{-3/2}}{J} = \frac{K_0}{J(1+10AJ)^{3/2}}, \qquad (38)$$

where A is

$$A \equiv \frac{Ri}{J} = \left(\frac{g}{\rho}\right)\left(\frac{\partial v}{\partial\rho}\right)^{-2}, \qquad (39)$$

and J again denotes the absolute value of the Jacobian.

Since we do not have estimates of $\partial v/\partial\rho$ for the unsmoothed density field we assume the minimum (subcritical) Ri value to be $Ri_s = 0.2$, at the center of the mixing region. We estimate the center J_s value from Figure 14a, as $J_s = 60$ m^4 kg^{-1}. The first equality in (38) (with $K_0 = 2.6 \times 10^{-3}$ m^2 s^{-1}) then gives $\delta = 8.3 \times 10^{-6}$ kg m^{-2} s^{-1}. Equation (39) gives $A = 0.0033$ kg m^{-4}, and $\partial v/\partial\rho = 1.7$ m^4 kg^{-1} s^{-1}. This last value is not much larger than the maximum value (1 m^4 kg^{-1} s^{-1}, see Figure 7b) estimated from the smoothed density field, as expected from our discussion at the end of section 4.1. As a first approximation, we assume that the calculated velocity gradient is constant and use (39) to obtain the Jacobian corresponding to $Ri_c = 0.25$, $J_c = Ri_c/A = 75$ m^4 kg^{-1}.

The value for β_1 is estimated (again from Figure 14a) to be $0.025\sigma_\theta$ units. The vertical Reynolds density flux distribution given by (37) (with the previously estimated δ and β_1) is shown in Figure 16a, together with the values of w_ρ and $\partial w_\rho/\partial\rho$, calculated from $w_\rho = -\partial(\overline{w'\rho'})/\partial z$ (equation (7)). The maxima of w_ρ and $\partial w_\rho/\partial\rho$ are approximately 5×10^{-6} kg m^{-3} s^{-1} and 5×10^{-4} s^{-1}, respectively. The maxima for w_d, estimated as $w_d = J_c w_\rho$, is 4×10^{-4} m s^{-1}.

The J distribution can now be calculated from (38), with the result shown by the solid line in Figure 17a. It shows a region of $J < J_c$ around the minimum, J_s. From an upper reference level, $\sigma_\theta(z = 270\text{ m}) = 26.58$, the J distribution can be integrated to give the density-depth variation shown in Figure 17b (solid line).

The most important result of these calculations is the large diapycnal convergence in the region of maximum vertical Reynolds density flux (see again Figure 16a). The convergence must push apart the well-packed isopycnal layers and compress the layers at the edges of the mixing region. In the central region, convergence reduces density fluctuations, eventually to zero

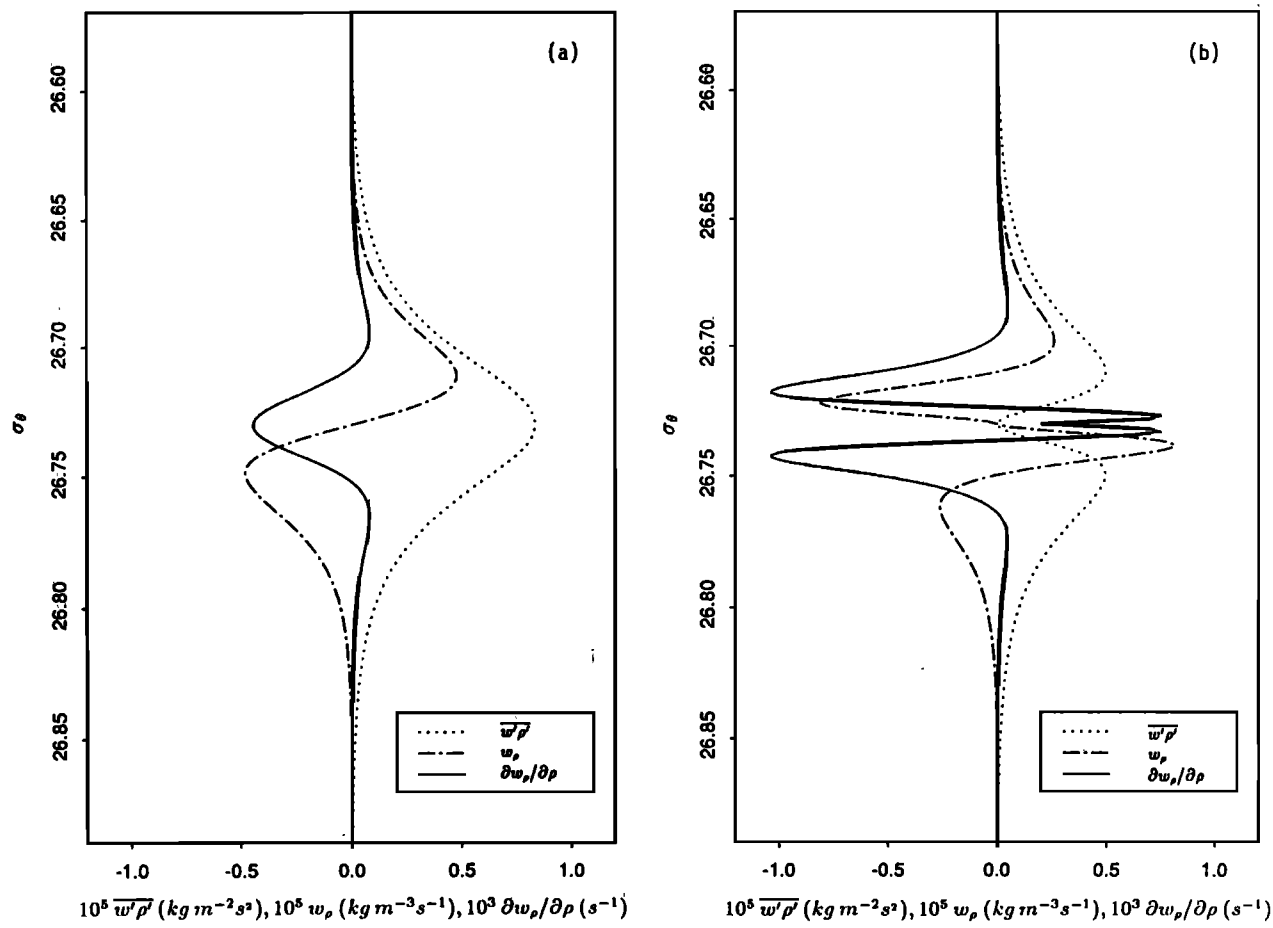

Figure 16. Simple model for the vertical Reynolds density flux, $\overline{w'\rho'}$, both (a) before and (b) after mixing. The dotted line is the hypothetical $\overline{w'\rho'}$ distribution, the dashed and solid lines the corresponding w_ρ and $\partial w_\rho/\partial\rho$ profiles.

once the layer is well-mixed, so that the density flux also drops to zero. Large enough convergence may generate secondary mixing events at the edges of the original mixing region. The modified density flux distribution, after secondary mixing at the edges, can be modeled by subtracting a second hyperbolic secant from the original one, of nearly the same amplitude, $\delta' = 0.999 \times 8.3 \times 10^{-6}$ kg m^{-2} s^{-1}, the factor 0.999 ensuring that no singularity develops. The second hyperbolic secant is taken to be narrower ($\beta_2 < \beta_1$), affecting only the region with $J < J_c$. The resulting distribution is

$$\overline{w'\rho'} = \delta\, sech\left[\frac{(\sigma_\theta - \sigma_m)}{\beta_1}\right] - \delta'\, sech\left[\frac{(\sigma_\theta - \sigma_m)}{\beta_2}\right]. \quad (40)$$

This, together with the corresponding w_ρ and $\partial w_\rho/\partial\rho$ distributions, is shown in Figure 16b. Following localized mixing, additional patches of positive and negative values of w_ρ and $\partial w_\rho/\partial\rho$ have been created.

With the modified $\overline{w'\rho'}$, we can again solve for J to obtain the results shown by the dotted-dashed line in Figure 17a. The subcritical J values have now disappeared, and a large peak in J has developed in their place. As before, we can calculate the modified density-depth variation (dotted-dashed line in Figure 17b). This shows the creation of a well-mixed region, a step in the density profile resembling those seen in Figure 14b.

Comparing Figure 16 with Figure 15, one sees evidence of primary mixing in the observations. Large peaks in the vertical Reynolds density flux, attributable to instability mixing, are accompanied by sidelobes of high diapycnal velocity, and opposing peaks of diapycnal convergence. The corresponding highly stratified layers are centered at $\sigma_\theta = 26.73$ and 27.08, while mixed layers would have developed at the edges of these stratified layers. The much smaller amplitude of the observed quantities is presumably due to the smoothing of the depth distribution. As discussed after Figure 14, other mixing mechanisms are likely to exist.

A rough estimate of how long mixing episodes may last can be obtained from (22) for the material tendency of j. For constant $\partial w_\rho/\partial\rho$, along a material trajectory this equation has a solution of the form

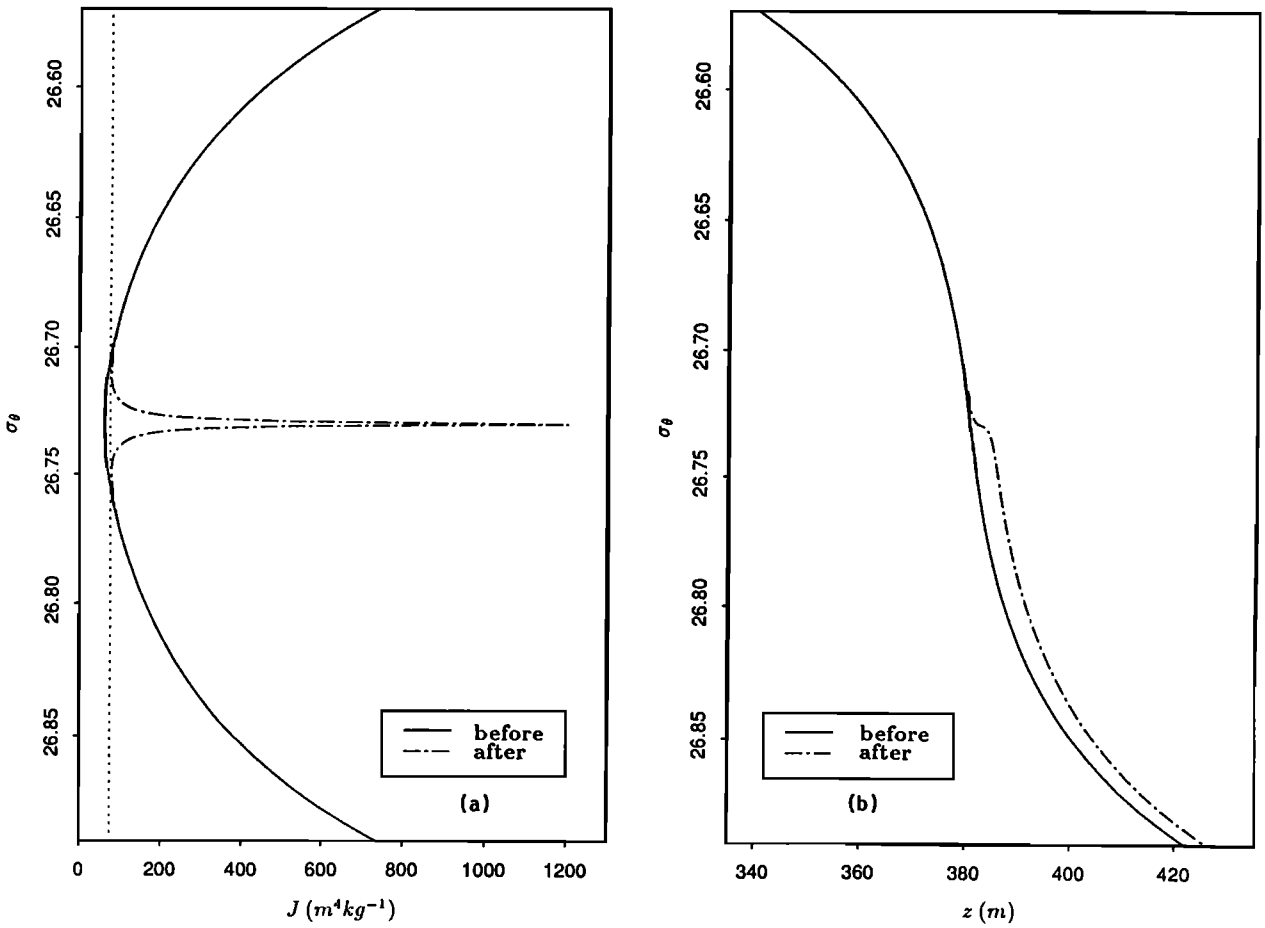

Figure 17. (a) Jacobian, J, and (b) depth, z, profiles corresponding to the original (before mixing, solid line) and modified (after mixing, dotted-dashed line) vertical Reynolds density flux $\overline{w'\rho'}$. The dotted vertical line in the Jacobian distribution indicates the value of J_c.

$$j \simeq j_0 \, exp\left(-\frac{\partial w_\rho}{\partial \rho} t\right). \tag{41}$$

With a value for $\partial w_\rho / \partial \rho$ of $O(10^{-4}\ s^{-1})$, we find that the anomaly in j (a factor of 5) would disappear in a few hours. Such a short timescale points at the ephemeral nature of any individual dynamical anomaly in the Gulf Stream and is consistent with our earlier assumption that mixing occurs in periods much shorter than the movements of the boundary current.

We showed earlier (Figure 11) that the two terms in (13), w_ρ^r and w_ρ^j, have the same sign in their contribution to w_ρ. This is because the direction of decreasing absolute value of J (positive w_ρ^j) is also the direction of increasing diapycnal shear and decreasing Ri (positive w_ρ^r). The resulting diapycnal convergence forces the isopycnals apart, increasing J. As the layers widen, the Richardson number goes well above critical. The result of this event is the generation of mixed, steplike, layers. With local values for w_d of $O(10^{-4}\ m\ s^{-1})$, and a timescale of several hours, we may estimate that during each mixing event a few meters of water are transferred into the subcritical (well-stratified) layers.

After many mixing events, occurring at different times and positions of the upper thermocline, the probable aggregate result is two-way exchange between adjacent layers. To sustain this process, the isopycnal layers must be drained or replenished through epipycnal divergence/convergence. One possible mechanism for this is through the correlation of layer depth and cross-stream velocity, or horizontal Reynolds mass flux (the "peristaltic pumping" suggested by *Csanady* [1989]), which is comprised under the C term in (21). Based on energy considerations, Csanady showed that this flux has to be necessarily convergent (negative) in the upper thermocline layers of a western boundary current.

6. The Upper Level Atmospheric Jet Stream Analogy

The similarity of tropospheric jet streams and oceanic currents has long been appreciated [*Iselin*, 1950; *Rossby*, 1951]. *Newton* [1978] compared the dimensions and volume transport profiles of the jet stream to those of the Gulf Stream. The similarity he found in volume trans-

port profile is remarkable, where the ratio of typical dimensions ranges from 1, for shear-related quantities, to 30, for horizontal size and velocity. Newton also noted that Gulf Stream meanders are dynamically similar to jet stream waves. He suggested that isentropic convergence, intensified diapycnal shear and downwelling at the troughs of jet stream waves and their counterparts at ridges, should be mirrored in the Gulf Stream. Many of these features can now indeed be identified, as shown by *Bower* [1989] and *Bower and Rossby* [1989].

The upper level frontal systems have been held responsible for mixing of tropospheric and stratospheric air masses. In the 1950s and 1960s this generated much interest in connection with the fate of radioactivity released by nuclear testing in the stratosphere. Later, attention turned to the transfer of chlorofluoromethanes from the troposphere to the stratosphere. In the ocean, western boundary currents play a similar role in the exchange of water masses of the continental margins with the ocean interior. The desire to understand that process was initially the principal motivation for our work.

Among the studies of the 1970s on the upper level jet stream, those relevant to the present work are *Shapiro*'s [1976, 1978] and *Gidel and Shapiro*'s [1979]. A review is given by *Keyser and Shapiro* [1986]; see also *Keyser and Rotunno* [1990]. *Shapiro* [1976] reported anomalously high potential vorticities in the upper level jet stream and, in order to explain them, postulated an appropriate distribution of turbulence and vertical Reynolds potential temperature flux (Figure 18). Later, in order to support his ideas, *Shapiro* [1978] showed more detailed distributions of Ri and q on a cross section of the upper level jet stream (Figure 19).

A comparison of Figure 19 with Figures 7a and 9b shows compelling similarity between the Ri and q anomalies in the jet stream and the Gulf Stream. The main difference between the two potential vorticity distributions arises because the jet stream has shear layers both above and below the level of maximum wind, while in western boundary currents the maximum velocity usually occurs near the sea surface. Hence in the oceanic case the vertical Reynolds density flux distribution, $\overline{w'\rho'}$, is similar to the lower half of the (negative) vertical Reynolds potential temperature flux, $-\overline{w'\theta'}$, shown in Figure 18b. The vertical density flux is zero at the sea surface if air-sea fluxes of heat and salt vanish, not because the velocity has a maximum as in the case of the jet stream.

Shapiros's concept of the mechanism responsible for the anomalies differs from ours. His approach is based on the following approximate relations in isentropic coordinates, with potential temperature θ as the vertical coordinate [*Shapiro*, 1976, equations (8) and (7)]:

$$\frac{d}{dt}\left[(\zeta+f)\frac{\partial\theta}{\partial p}\right] \simeq (\zeta+f)\frac{\partial}{\partial p}\left(\frac{d\theta}{dt}\right), \qquad (42)$$

$$\frac{d\theta}{dt} \simeq -\frac{\partial(\overline{w'\theta'})}{\partial z}, \qquad (43)$$

where d/dt is identical to $\mathcal{D}/\mathcal{D}t$ but with θ replacing ρ. Shapiro suggested that high potential vorticity anomalies are produced at the level of maximum wind, through mixing by clear air turbulence. He said that this inhibits the vertical spreading of the isentropes during frontogenesis, required in a cyclonic shear zone by conservation of potential vorticity.

The last two equations, together with the potential temperature flux distribution postulated by *Shapiro* [1976] (reproduced here as Figure 18b), indeed suggest that a region of high potential vorticity may be gener-

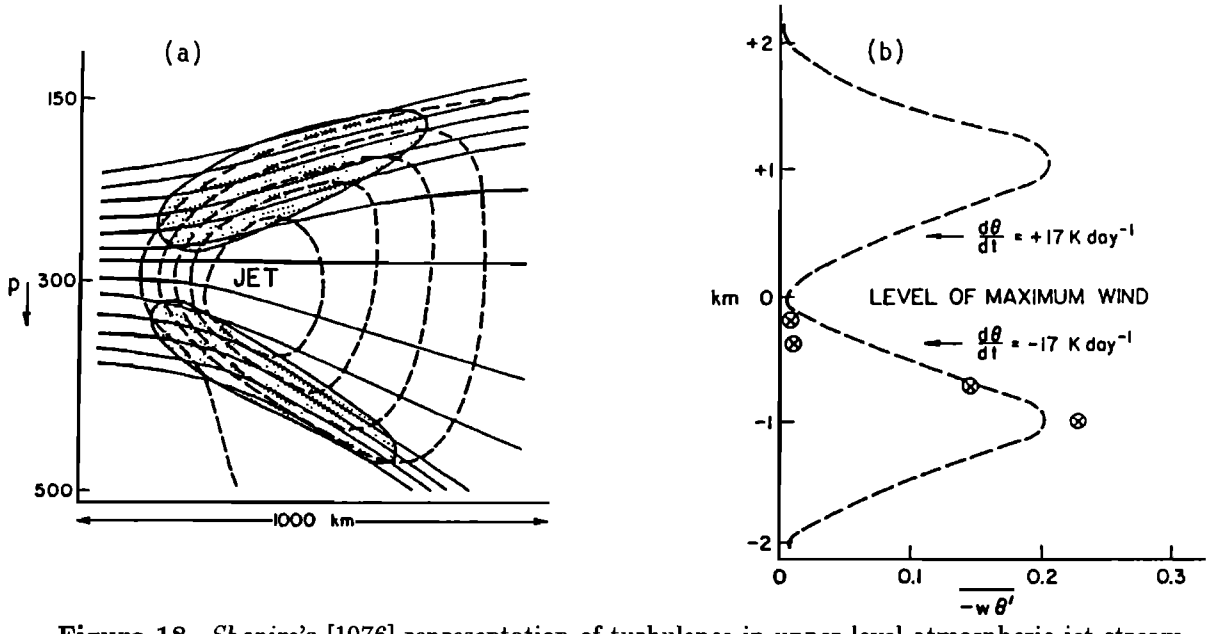

Figure 18. *Shapiro*'s [1976] representation of turbulence in upper level atmospheric jet stream systems. (a) Regions of clear-air turbulence in the vicinity of the jet stream are stippled; the solid and dashed lines are contours of potential temperature and wind speed, respectively. (b) The postulated vertical Reynolds potential temperature flux, $\overline{w'\theta'}$, is shown as a function of height; the crosses indicate observed values.

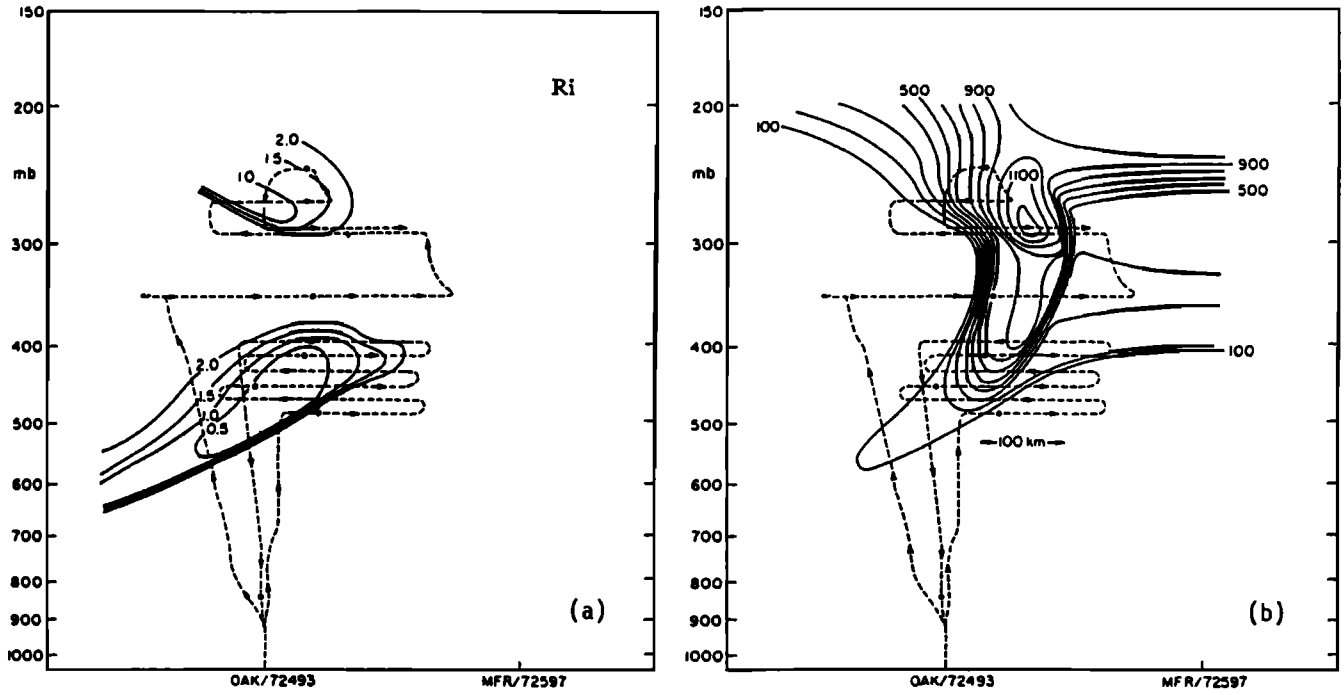

Figure 19. (a) Richardson number and (b) potential vorticity (in units of 10^{-7} K s^{-1} $mbar^{-1}$), in isobaric coordinates, for a section across the upper level atmospheric jet stream system (reproduced from *Shapiro* [1978]). The dashed line indicates the flight path taken during the observations.

ated at the level of maximum wind (note again that we talk in terms of absolute values; actually, $(\zeta + f)\,\partial\theta/\partial p$ is negative and $\partial/\partial p\,(d\theta/dt)$ is a negative maximum at the level of maximum wind). However, from the same argument, regions of low potential vorticity should arise at the maxima in vertical shear, the two maxima of $-\overline{w'\theta'}$ in Figure 18b. This is not the case in Figure 19b, with q being large precisely where, according to Shapiro's criterion, it should be small.

Equations (42) and (43) are essentially the same as our (32) and $w_\rho \simeq -\partial(\overline{w'\rho'})/\partial z$ (see equation (7)). Equation (32) may be rewritten as

$$\frac{\mathcal{D}}{\mathcal{D}t}\left[\frac{(\zeta + f)}{\rho}\frac{\partial \rho}{\partial z}\right] \simeq \frac{(\zeta + f)}{\rho}\frac{\partial w_\rho}{\partial z}. \qquad (44)$$

Note that (42) and (44) are equivalent, except for the density, ρ, which (44) retains inside the material derivative. This difference arises from the definitions of potential vorticity used by Shapiro and here (the terms between brackets in (42) and (44), respectively). Equation (44) can actually be rewritten as (42) with the appearance of additional terms, which Shapiro assumed to be negligible besides the diapycnal divergence term. Note also that (42) has derivatives with respect to pressure, while (44) has them with respect to depth, which compensates for θ and ρ increasing in opposite vertical directions (in particular, $\overline{w'\theta'}$ is negative and $\overline{w'\rho'}$ positive).

Our interpretation is that mixing is triggered by the dense packing of isopycnals (regions of low J and high q values) during frontogenesis, while diapycnal shear is maintained or increased. From this point of view the low J (and high q) values are the results of frontogenesis, and mixing that reduces the anomalies is the consequence. As we have argued above, a simple model as well as observations support this point of view. Figure 13 shows that anomalously small j (high q) values are associated with diapycnal convergence, not divergence as Shapiro's ideas would imply. The same point of view underlies the analyses by *Roach* [1970] and *Browning et al.* [1970] of atmospheric jet streams, who assumed that a critical Ri number limits the vertical spacing between isentropes during frontogenesis.

One way to reconcile the q distribution in the Gulf Stream with Shapiro's observations for the jet stream is to note that in Figure 19b there could actually be two distinct maxima of q, if the single maximum were an artifice of contouring over the relatively poorly sampled level of maximum wind. This would then agree with two observed separate minima in Ri (Figure 19a). In this manner the similarity between one-half of the upper level frontal system and the western boundary frontal system would be complete.

7. Conclusions

Isopycnic coordinates are powerful in the analysis of anomalies produced by diapycnal mass transfer in western boundary currents. Anomalies may occur in the distribution of tracers, such as nutrients, and in dynamical quantities that control the structure of the flow, such as the Jacobian or potential vorticity. In a hydrographic

section off the Mid-Atlantic Bight we find substantial anomalies in the upper thermocline layers of the Gulf Stream for all these quantities. The anomalies coexist with small (but not subcritical) Richardson numbers, calculated from smoothed data. The raw data show much sharper gradients, but also density inversions, which have to be eliminated in order to define the isopycnic coordinate system. It is reasonable to suppose, however, that unsmoothed Richardson numbers are locally and temporally subcritical.

We establish theoretically that coincident anomalies of small Jacobian and large potential vorticity imply dominant diapycnal convergence (or divergence), causing thicker (or thinner) isopycnal layers. The density tendency (and hence the diapycnal velocity) is calculated from the vertical gradient of the Reynolds density flux, parameterized in terms of the Jacobian and the Richardson number. This model allows us to resolve that diapycnal convergence (and not divergence) is associated with the observed anomalies in Jacobian and potential vorticity. Our interpretation is that highly packed isopycnal layers start spreading apart through inflow (convergence) from the adjacent isopycnal layers.

We hypothesize that frontogenesis in meanders causes a reduction of the Jacobian, while the diapycnal gradients of the horizontal velocities remain constant or increase, which occasionally takes the Richardson number below its critical value. This produces mixing between adjacent layers of fluid, raising or lowering isopycnals. The (temporal and spatial) aggregate result is two-way water exchange between adjacent layers of western boundary currents. Our crude estimate for the maximum diapycnal velocity is 4×10^{-4} m s^{-1}. This is large enough to account for the overall two-way exchange coefficient between the upper thermocline and surface layers of the Gulf Stream, calculated in PC from mass and nutrient balances (2×10^{-5} m s^{-1}).

An important concept arising from our analysis is *Ri* control of mixing in western boundary currents. According to this concept, adjacent isopycnals can only approach each other up to a certain point, at which *Ri* becomes critical. Instability then creates well-mixed regions, or steps, in the density-depth profile. A simple model of diapycnal mass transfer associated with mixing in unstable layers, akin to *Phillips* [1972] mechanistic model, is able to reproduce the observed steps.

High and low J regions are responsible for the patchy character of the diapycnal velocity field in the Gulf Stream. This field, consisting of alternating positive and negative diapycnal velocities, causes localized diapycnal divergence and convergence (with packing and spreading of the isopycnals). Thus diapycnal velocities are not only a passive result of the diapycnal distribution of the horizontal velocities and of the small-scale structure of the layers but are responsible for modifying this structure and the distribution of potential vorticity.

Diapycnal divergence and convergence can locally dominate the potential vorticity balance within the upper thermocline Gulf Stream, the relevant term being 3 orders of magnitude greater than the contribution from the planetary vorticity gradient. On the other hand, vertical averaging over even relatively short distances (16 m) rapidly reduces the calculated diapycnal convergence, to the point where its effect on the vorticity balance is of the same order as planetary vorticity. Its importance in the overall potential vorticity balance is a question that must be left open.

The resemblance between the present work and *Shapiro*'s [1976, 1978] analysis of the upper level atmospheric jet stream is noteworthy. However, the interpretation of the two sets of observations is different. In our model frontogenesis is the origin of the anomalies, and mixing, once a critical *Ri* is attained, is their consequence, while according to Shapiro the anomalies are the result of mixing by clear air turbulence.

Our results uphold *Stommel*'s [1965, p. 116] hypothesis of localized intense diapycnal mixing in the upper thermocline layers of the Gulf Stream: "... the real Gulf Stream approaches critical internal Froude flow, and it is quite conceivable that as a result there are internal hydraulic jumps and other interesting small-scale phenomena, such as oblique shock fronts, along the left-hand, inshore edge of the Stream." We believe that our results also show the potential application of isopycnic analysis in fine-scale studies, particularly in studying the causes and consequences of shear-driven mixing.

Appendix A: Errors Using $\phi = p/\rho + gz$

McDougall [1989] has clearly shown that $\phi = p/\rho + gz$ is a stream function on constant in situ density surfaces, but not on isopycnals. The expression for ϕ may be compared with the (true) Montgomery potential [*Montgomery*, 1937] on surfaces of constant specific volume anomaly (steric anomaly), $\delta = 1/\rho - 1/\rho(35, 0, p)$. This exact stream function on steric anomaly surfaces is defined as $\phi_M = p\delta - \int_{p_r}^{p} \delta dp$, with p_r the reference pressure. *McDougall* [1989] has suggested the utilization of this potential on steric anomaly surfaces as a viable alternative to stream functions on neutral surfaces. *Zhang and Hogg* [1992] have shown, for a particular case, that using ϕ_M on isopycnals also gives relatively small errors. In general, however, the error will depend on the case under consideration, and both *McDougall* [1989] and *Zhang and Hogg* [1992] have suggested different ways to optimize the potentials.

For our case we may easily show that ϕ is very adequate to calculate diapycnal and epipycnal shears. To do so we follow *McDougall* [1989, equation (24)], who obtained an expression for the error produced when using ϕ to calculate the velocity difference between two neutral surfaces. As discussed in section 2, in our case the isopycnals and neutral surfaces are very similar, so we can estimate this error as

$$\epsilon \simeq -\frac{g^2 z_1}{c_1^2}\frac{\partial z}{\partial x}\bigg|_1 + \frac{g^2 z_2}{c_2^2}\frac{\partial z}{\partial x}\bigg|_2$$

$$\epsilon \simeq \frac{g^2(z_2 - z_1)}{\bar{c}^2}\overline{\frac{\partial z}{\partial x}}, \qquad \text{(A1)}$$

where the subindexes 1 and 2 identify the two isopycnals, c is the speed of sound in seawater, and the overbars represent the average of the two values at the isopycnals. The last approximation is possible because the water speed changes very little (by about only 1%) over the region of consideration and because all isopycnals in the upper thermocline have similar slopes across the Gulf Stream.

The difference $(z_2 - z_1)$ gives precisely the distance over which we will estimate the vertical gradients. Hence the error in estimating the diapycnal shear is

$$\frac{\partial \epsilon}{\partial \rho} = J \frac{\partial \epsilon}{\partial z} \simeq \frac{g^2 J}{\bar{c}^2} \frac{\overline{\partial z}}{\partial x} \cdot \tag{A2}$$

Using $\bar{c} \simeq 1500$ m s^{-1}, $\overline{\partial z/\partial x} \sim 5 \times 10^{-3}$ (Figure 5a), and $J \sim 5 \times 10^2$ m^4 kg^{-1} (Figure 5b) gives $\partial \epsilon/\partial \rho \sim 10^{-4}$ m^4 kg^{-1} s^{-1}. This is insignificant when compared with typical values $\partial v/\partial \rho \simeq 0.7$ m^4 kg^{-1} s^{-1} (Figure 7b).

The error in our estimate for the epipycnal shear is

$$\begin{aligned} \frac{\partial \epsilon}{\partial x} &= \left.\frac{\partial \epsilon}{\partial x}\right|_z + \frac{\partial z}{\partial x}\frac{\partial \epsilon}{\partial z} \\ \frac{\partial \epsilon}{\partial x} &\simeq \frac{g^2(z_2 - z_1)}{\bar{c}^2} \frac{\partial}{\partial x}\left(\frac{\overline{\partial z}}{\partial x}\right)_z + \frac{\partial z}{\partial x}\frac{\partial \epsilon}{\partial z} \cdot \end{aligned} \tag{A3}$$

The first term on the right-hand side of this equation is negligible because the slope of isopycnals (at a constant level) changes little within the upper thermocline layers of the Gulf Stream (and even less the average slope of two close isopycnals). Using $\partial \epsilon/\partial z \sim 2 \times 10^{-7}$ s^{-1} (from above) and $\partial z/\partial x \sim 5 \times 10^{-3}$, gives $\partial \epsilon/\partial x \sim 10^{-9}$ s^{-1}, much smaller than the typical value $\partial v/\partial x \sim 10^{-5}$ s^{-1} (Figure 9a).

Appendix B: Validity of Approximations (22) and (32)

To support the goodness of our estimates, we need to establish that shear-induced mixing may dominate the mass and potential vorticity balances within the upper thermocline layers of the Gulf Stream, i.e., we must show the accuracy of approximations (22) and (32).

Let us first look at the validity of (32). To do so we need estimates for tilting of horizontal vorticity and torque by eddy stresses. Table B1 summarizes the magnitude of various quantities within the Gulf Stream, both from the smoothed density data of section 36N (top row) and from the model of diapycnal mass transfer discussed in section 5 (bottom row). We may estimate the tilting term in (31) from

$$\frac{T_i}{j} \simeq -\frac{1}{j}\frac{\partial w_\rho}{\partial x}\frac{\partial v}{\partial \rho} \cdot \tag{B1}$$

Using the smoothed data (numbers in the top row of Table B1), this gives a maximum absolute value $T_i/(jq) \sim 1.1 \times 10^{-9}$ s^{-1}. Similarly, the torque term may be estimated from

$$\frac{T_o}{j} \simeq \frac{1}{j}\frac{\partial B}{\partial x} \sim \frac{A_v}{j}\frac{\partial}{\partial x}\left(\frac{\partial^2 v}{\partial z^2}\right) + \frac{A_h}{j}\frac{\partial}{\partial x}\left(\frac{\partial^2 v}{\partial x^2}\right), \tag{B2}$$

where A_v and A_h are the vertical and horizontal eddy viscosity coefficients. Let us call the first term on the right, depending on A_v, T_{ov}/j, and the second, depending on A_h, T_{oh}/j. The along-stream velocity, cross-stream length and depth scales can be set as 1 m s^{-1}, 25 km and 500 m, respectively. Using these scales, and assuming $A_v \simeq K$ and $A_h \simeq 300$ m^2 s^{-1} [*Bower et al.*, 1985; *Boudra and Chassignet*, 1988], we obtain $T_{ov}/(jq) \sim 2.1 \times 10^{-11}$ s^{-1} and $T_{oh}/(jq) \sim 1.9 \times 10^{-7}$ s^{-1}. Note that only the first value is entered in the top row in Table B1, which lists the vertically smoothed estimates. The second value, which depends solely on epipycnal gradients, is not affected by smoothing, and is entered only in the bottom row, along with the estimates using the unsmoothed data: it would clearly not be appropriate to compare it with the highly damped estimates of the top row. The maximum value of $\partial w_\rho/\partial \rho$ for the smoothed density field is 1.1×10^{-7} s^{-1} (Figure 13a). This value is much larger than both tilting and the contribution of vertical eddy diffusion to the torque.

The bottom row of Table B1 lists the estimates obtained from the idealized (unsmoothed) model discussed in section 5, with the help of the above scales. The maximum tilt and torque contributions to the potential vorticity equation are now several orders of magnitude larger than those in the top row. However, they are still considerably smaller than our new estimate for the diapycnal convergence, 5×10^{-4} s^{-1}. The next term in size is tilting of horizontal vorticity, 2 orders of magnitude smaller.

Table B1. Estimates for Quantities Involved in Maximum Contributions to the Potential Vorticity and Mass Balances Within the Upper Thermocline Layers of the Gulf Stream

j,	q,	$\partial w_\rho/\partial x$,	$\partial v/\partial \rho$,	K,	$T_i/(jq)$,	$T_{ov}/(jq)$,	$T_{oh}/(jq)$,	w_ρ,	w_e,	$\partial w_\rho/\partial \rho$,
10^4	10^{-10}	10^{-13}		10^{-5}	10^{-9}	10^{-11}	10^{-7}	10^{-9}	10^{-7}	10^{-7}
m	(m s)$^{-1}$	kg/(m^4 s)	m^4/(kg s)	m^2/s	s^{-1}	s^{-1}	s^{-1}	kg/(m^3 s)	m/s	s^{-1}
20	5	1.1	1	1.3	1.1	2.1	-	2.6	6.6	1.1
7.5	12	2000	1.7	40	4000	6000	1.9	5000	4000	5000

The top row gives the results as calculated from the 16-m-smoothed density data. The bottom row gives estimates from the unsmoothed data together with results from the simple model of diapycnal mass transfer.

The importance of the diapycnal term in (31) may be further highlighted by comparing it with the relative change of planetary vorticity due to advection, $(v/f)(\partial f/\partial y)$. For $v = 1\,m\ s^{-1}$ this term is 2.1×10^{-7} s^{-1}, 3 orders of magnitude smaller than the maximum diapycnal divergence. This indicates that, within the Gulf Stream, localized stretching or shrinking can indeed dominate vorticity changes. The situation is different for the vertically smoothed values, however, with both terms being of similar magnitude. This shows that what appears as little vertical averaging (a 16-m running filter) may produce a large reduction in the local values of diapycnal divergence or convergence.

We turn now at the question of the validity of (22); to answer it we need estimates for the epipycnal divergence and the horizontal Reynolds mass flux. *Bower* [1989] estimated the contribution of epipycnal divergence to the potential vorticity balance (this term is clear if we substitute (21) into (33)). She did so by calculating the relative change in absolute vorticity between the initial and final positions of isopycnic Lagrangian drifters (RAFOS floats), under the assumption that potential vorticity is conserved along an isopycnal trajectory. Here we have shown that within the Gulf Stream this assumption may be incorrect, with Jacobian anomalies considerably larger than those of the absolute vorticity. The RAFOS floats are designed for self-adjusting compressibility [*Bower and Rossby*, 1989] and cannot follow diapycnal mixing. Nevertheless, Bower's estimates, obtained from an ensemble of trajectories which presumably average out the local effects of diapycnal mixing, are likely to be of the correct order of magnitude. The mean values she obtained for epipycnal divergence are about $(\pm)\ 5 \times 10^{-7}\ s^{-1}$. Again, these epipycnal estimates must be compared with those from our model for the unsmoothed density field. In doing so we see that the epipycnal divergence is 3 orders of magnitude smaller than the estimated maximum contribution from the diapycnal convergence.

Finally, the horizontal Reynolds mass flux contribution to the mass balance may be estimated using *Csanady*'s [1989] parameterization for western boundary currents. This is based on the idea that the depth and velocity fluctuations must be proportional to the characteristic layer depth and mean velocity of the current (v_m), which can be written as $\overline{u'j'} \sim \alpha j v_m$, where $\alpha \simeq 0.0025$. The corresponding term in (21) would be

$$\rho C \simeq \frac{\partial(\overline{u'j'})}{\partial x} \sim \frac{\partial(\alpha j v_m)}{\partial x} \qquad \text{(B3)}$$

With typical values for the upper thermocline layers of the Gulf Stream, we can estimate the order of magnitude of the appropriate term for comparison with diapycnal convergence in (22), $(\rho C)/j \sim 10^{-7}\ s^{-1}$. This term is again much smaller than the diapycnal term for the unsmoothed model. This result could have been expected in view of equation (33), which shows that the horizontal Reynolds mass fluxes must be related with the horizontal Reynolds stresses. Hence its contribution should be similar to the $T_o/(jq)$ term discussed above.

Acknowledgments. We are grateful to Mike McCartney for providing the hydrographic data and to Jenifer Clark for making available the frontal analysis maps. We are thankful to Larry Atkinson, John Bane and Denny Kirwan for their comments to the original version of this paper. We are also grateful to our two reviewers, for their careful reading of the manuscript and their comments on the "pesky compressible nature of seawater" and the interpretation of "finescale evidence." This work has been supported by the Department of Energy under a grant entitled "The role of the continental margin processes in the nutrient bearing strata of the North Atlantic," and by the Commonwealth Center for Coastal Physical Oceanography.

References

Armi, L., Effects of variations in eddy diffusivity on property distributions in the oceans, *J. Mar. Res., 37,* 515-530, 1979.

Bane, J. M., Jr. , D. A. Brooks, and K. R. Lorenson, Synoptic observations of the three-dimensional structure and propagation of Gulf Stream meanders along the Carolina continental margin, *J. Geophys. Res., 86,* 6411-6425, 1981.

Bleck, R., Finite difference equations in generalized vertical coordinates, 1, Total energy conservation, *Contrib. Atmos. Phys., 51,* 360-372, 1978.

Bleck, R., Finite difference equations in generalized vertical coordinates, 2, Potential vorticity conservation, *Contrib. Atmos. Phys., 52,* 95-105, 1979.

Bleck, R., On the conversion between mean and eddy components of potential and kinetic energy in isentropic and isopycnic coordinates, *Dyn. Atmos. Oceans, 9,* 17-37, 1985.

Bleck, R., and D. Boudra, Wind-driven spin-up in eddy-resolving ocean models formulated in isopycnic and isobaric coordinates, *J. Geophys. Res., 91,* 7611-7621, 1986.

Bleck, R., R. Onken, and J. D. Woods, A two-dimensional model of mesoscale frontogenesis in the ocean, *Q. J. R. Meteorol. Soc., 114,* 347-371, 1988.

Boudra, D. B., and E. P. Chassignet, Dynamics of Agulhas retroflection and ring formation in a numerical model, 1, The vorticity balance, *J. Phys. Oceanogr., 18,* 280-303, 1988.

Bower, A. S., Potential vorticity balances and hotizontal divergence along particle trajectories in Gulf Stream meanders east of Cape Hatteras, *J. Phys. Oceanogr., 19,* 1669-1681, 1989.

Bower, A. S., and T. Rossby, Evidence of cross-frontal exchange processes in the Gulf Stream based on isopycnal RAFOS float data, *J. Phys. Oceanogr., 19,* 1177-1190, 1989.

Bower, S. A., H. T. Rossby, and J. L. Lillibridge, The Gulf Stream - Barrier or blender?, *J. Phys. Oceanogr., 15,* 24-32, 1985.

Browning, K. A., T. W. Harrold, and J. R. Starr, Richardson number limited shear zones in the free atmosphere, *Q. J. R. Meteorol. Soc., 96,* 40-49, 1970.

Chereskin, T. K., J. N. Moum, P. J. Stabero, D. R. Caldwell, C. A. Paulson, L. A. Regier, and D. Halpern, Time scale variability at 140° W in the equatorial Pacific, *J. Geophys. Res., 91,* 12887-12897, 1986.

Csanady, G. T., Energy dissipation and upwelling in a western boundary current, *J. Phys. Oceanogr., 19,* 462-473, 1989.

Csanady, G. T., Mixing in coastal regions, in *The Sea: Ocean Engineering Science,* vol. 9, edited by B. Le Mehaute and D. M. Hanes, pp. 593-629, John Wiley, New York, 1990.

Csanady, G. T., and P. Hamilton, Circulation of slopewater, *Cont. Shelf Res., 8,* 565-624, 1988.

Deardorff, J. W., Empirical dependence of the eddy coefficient for heat upon stability above the lowest 50 m, *J. Appl. Meteorol., 6,* 631-643, 1967.

Deardorff, J. W., A multi-limit mixed-layer entrainment formulation, *J. Phys. Oceanogr., 13,* 988-1002, 1983.

deSzoeke, R. A., On the effects of horizontal variability of wind stress on the dynamics of the ocean mixed layer, *J. Phys. Oceanogr., 10,* 1439-1454, 1980.

Dutton, J. A., *The Ceaseless Wind,* 579 pp., McGraw-Hill, New York, 1976.

Ellison, T. H., Turbulent transport of heat and momentum from an infinite rough plane, *J. Fluid Mech., 2,* 456-466, 1957.

Eriksen, C. C., Measurements and models of fine structure, internal gravity waves and wave breaking in the deep ocean, *J. Geophys. Res., 83,* 2989-3009, 1978.

Eriksen, C. C., Observations of the seasonal cycle of upper ocean structure and the roles of advection and diapycnal mixing, *J. Geophys. Res., 92,* 5354-5368, 1987.

Fernando, H. J. S., Turbulent mixing in stratified fluids, *Annu. Rev. Fluid Mech., 23,* 455-493, 1991.

Foo, E., A two-dimensional diabatic isopycnic model-simulating the coastal upwelling front, *J. Phys. Oceanogr., 11,* 604-626, 1981.

Gargett, A. E., Vertical eddy diffusivity in the ocean interior, *J. Mar. Res., 42,* 359-393, 1984.

Garrett, C., On the parameterization of diapycnal fluxes due to double-diffusive intrusions, *J. Phys. Oceanogr., 12,* 952-959, 1982.

Gaspar, P., Modeling the seasonal cycle of the upper ocean, *J. Phys. Oceanogr., 18,* 161-180, 1988.

Gibson, C. H., Fossil turbulence and intermittency in sampling oceanic mixing processes, *J. Geophys. Res., 92,* 5383-5404, 1987.

Gidel, L. T., and M. A. Shapiro, The role of clear air turbulence in the production of potential vorticity in the vicinity of upper tropospheric jet stream-frontal systems, *J. Atmos. Sci., 36,* 2125-2138, 1979.

Gregg, M. C., Diapycnal mixing in the thermocline: A review, *J. Geophys. Res., 92,* 5249-5286, 1987.

Gregg, M. C., and T. B. Sanford, Signatures of mixing from the Bermuda Slope, the Sargasso Sea and the Gulf Stream, *J. Phys. Oceanogr., 10,* 105-127, 1980.

Gregg, M. C., E. A. D'Asaro, T. J. Shay, and N. Larson, Observations of persistent mixing and near-inertial internal waves, *J. Phys. Oceanogr., 16,* 856-885, 1986.

Hamilton, P., and M. Rattray Jr., A numerical model of the depth-dependent wind-driven upwelling circulation on a continental shelf, *J. Phys. Oceanogr., 8,* 437-457, 1978.

Haynes, P. H., and M. E. McIntyre, On the evolution of vorticity and potential vorticity in the presence of diabatic heating and frictional or other forces, *J. Atmos. Sci., 44,* 828-841, 1987.

Haynes, P. H., and M. E. McIntyre, On the conservation and impermeability theorems for potential vorticity, *J. Atmos. Sci., 47,* 2021-2031, 1990.

Hogg, N., P. Biscaye, W. Gardner, and W. J. Schmitz, Jr., On the transport and modification of Antarctic Bottom Water in the Vema Channel, *J. Mar. Res., 40,* suppl., 231-263, 1982.

Hopfinger, E. J., Turbulence in stratified fluids: A review, *J. Geophys. Res., 92,* 5287-5303, 1987.

Iselin, C.O., Some common characteristics of the Gulf Stream and the atmospheric jet stream, *Trans. N. Y. Acad. Sci., Ser. II, 13,* 84-86, 1950.

Itsweire, E. C., T. R. Osborn, and T. P. Stanton, Horizontal distribution and characteristics of shear layers in the seasonal thermocline, *J. Phys. Oceanogr., 19,* 301-320, 1989.

James, I. D., A model on the annual cycle of temperature in a frontal region of the Celtic Sea, *Estuarine Coastal Mar. Sci., 5,* 339-353, 1977.

James, I. D., A note on the circulation induced by a shallow-sea front, *Estuarine Coastal Mar. Sci., 7,* 197-202, 1978.

Johnson, D. R., A generalized transport equation for use with meteorological coordinate systems, *Mon. Weather Rev., 108,* 733-745, 1980.

Kao, T. W., C. Park, and H. Pao, Buoyant surface discharge and small-scale oceanic fronts: A numerical study, *J. Geophys. Res., 82,* 1747-1752, 1977.

Keyser, D., and R. Rotunno, On the formation of potential-vorticity anomalies in upper-level jet-front systems, *Mon. Weather Rev., 118,* 1914-1921, 1990.

Keyser, D., and M. A. Shapiro, A review of the structure and dynamics of upper-level frontal zones, *Mon. Weather Rev., 114,* 452-499, 1986.

Komori, S., H. Ueda, F. Ogino, and T. Mizushina, Turbulence structure in stably stratified open-channel flow, *J. Fluid. Mech., 130,* 13-26, 1983.

Kullenberg, G., C. R. Murthy, and H. Westerberg, Vertical mixing characteristics in the thermocline and hypolimnion regions of Lake Ontario (IFYGL), *Proc. Conf. Great Lakes Res., 17,* 425-434, 1974.

Kundu, P. K., and R. C. Beardsley, Evidence of a critical Richardson number in moored measurements during the upwelling season off Northern California, *J. Geophys. Res., 96,* 4855-4868, 1991.

Kunze, E., A. J. Williams III, and M. G. Briscoe, Observations of shear and vertical stability from a neutrally buoyant float, *J. Geophys. Res., 95,* 18127-18142, 1990.

Leaman, K. D., E. Johns, and T. Rossby, The average distribution of volume transport and potential vorticity with temperature at three sections across the Gulf Stream, *J. Phys. Oceanogr., 19,* 36-51, 1989.

Lietzke, T. A., and A. Lerman, Effects of bottom relief in two-dimensional oceanic eddy diffusion models, *Earth Planet. Sci. Lett., 24,* 337-344, 1975.

Luyten, J., J. Pedlosky, and H. Stommel, The ventilated thermocline, *J. Phys. Oceanogr., 13,* 292-309, 1983.

Marmorino, G. O., Observations of small-scale mixing processes in the seasonal thermocline, 2, Wave breaking, *J. Phys. Oceanogr., 17,* 1348-1355, 1987.

McDougall, T. J., The relative roles of diapycnal and isopycnal mixing on subsurface water mass conversion, *J. Phys. Oceanogr., 14,* 1577-1589, 1984.

McDougall, T. J., Thermobaricity, cabbeling, and water-mass conversion, *J. Geophys. Res., 92,* 5448-5464, 1987a.

McDougall, T. J., Neutral surface, *J. Phys. Oceanogr., 17,* 1950-1964, 1987b.

McDougall, T. J., Neutral-surface potential vorticity, *Prog. Oceanogr., 20,* 185-221, 1988.

McDougall, T. J., Streamfunctions for the lateral velocity vector in a compressible ocean, *J. Mar. Res., 47,* 267-284, 1989.

McDougall, T. J., and Y. You, Implications of the nonlinear equation of state for upwelling in the ocean interior, *J. Geophys. Res., 95,* 13263-13276, 1990.

Miles, J., Richardson's criterion for the stability of stratified shear flow, *Phys. Fluids, 29,* 3470-3471, 1986.

Miller, J. L., and D. L. Evans, Density and velocity fine structure enhancement in oceanic eddies, *J. Geophys. Res., 90,* 4793-4806, 1985.

Montgomery, R. B., A suggested method for representing gradient flow in isentropic surfaces, *Bull. Am. Meteorol. Soc., 18,* 210-212, 1937.

Moum, J. N., and T. R. Osborn, Mixing in the main thermocline, *J. Phys. Oceanogr., 16,* 1250-1259, 1986.

Munk, W. H., and E. R. Anderson, Notes on a theory of the thermocline, *J. Mar. Res., 7,* 276-295, 1948.

Newton, C. W., Frontogenesis and frontolysis as a three-dimensional process, *J. Meteorol., 11,* 449-461, 1954.

Newton, C. W., Fronts and wave disturbances in Gulf Stream and atmospheric jet stream, *J. Geophys. Res., 83,* 4697-4706, 1978.

Palmén, E., and C. E. Newton, *Atmospheric circulation systems,* 603 pp., Academic, San Diego, Calif., 1969.

Pelegrí, J. L., and G. T. Csanady, Nutrient transport and mixing in the Gulf Stream, *J. Geophys. Res., 96,* 2577-2583, 1991.

Peters, H., M. C. Gregg, and J. M. Toole, On the parameterization of equatorial turbulence, *J. Geophys. Res., 93,* 1199-1218, 1988.

Phillips, O. M., Turbulence in a strongly stratified fluid-is it unstable?, *Deep Sea Res., 19,* 79-81, 1972.

Posmentier, E. S., The generation of salinity finestructure by vertical diffusion, *J. Phys. Oceanogr., 7,* 292-300, 1977.

Rhines, P. B., and W. Y. Young, A theory of wind-driven circulation, 1, Mid-ocean gyres, *J. Mar. Res., 40,* 559-596, 1982.

Roach, W. T., On the influence of synoptic development on the production of high level turbulence, *Q. J. R. Meteorol. Soc., 96,* 413-429, 1970.

Roemmich, D., and C. Wunsch, Two transatlantic sections: meridional circulation and heat flux in the subtropical North Atlantic Ocean, *Deep Sea Res., 32,* 619-644, 1985.

Rossby, C. G., On the vertical and horizontal concentration of momentum in air and ocean currents, *Tellus , 3,* 15-27, 1951.

Ruddick, B. R., T. J. McDougall, and J. S. Turner, The formation of layers in a uniformly stirred density gradient, *Deep Sea Res., 36,* 597-609, 1989.

Sarmiento, J. L., H. W. Feely, W. S. Moore, A. E. Bainbridge, and W. S. Broecker, The relationship between vertical eddy diffusion and buoyancy gradient in the deep sea, *Earth Planet. Sci. Lett., 32,* 357-370, 1976.

Shapiro, M. A., The role of turbulent heat flux in the generation of potential vorticity in the vicinity of upper-level jet stream systems, *Mon. Weather Rev., 104,* 892-906, 1976.

Shapiro, M. A., Further evidence of the mesoscale and turbulent structure of upper level jet stream-frontal zone system, *Mon. Weather Rev., 106,* 1100-1111, 1978.

Smethie, W. M., Jr., Estimation of vertical mixing rates in fjords using naturally occurring radon-222 and salinity as tracers, in *Fjord Oceanography,* edited by H. J. Freeland, D. M. Framer, and C. D. Levings, pp. 241-249, Plenum, New York, 1980.

Staley, D. O., Evaluation of potential-vorticity changes near the tropopause and the related vertical motions, vertical advection of vorticity, and transfer of radioactive debris from stratosphere to troposphere, *J. Meteorol., 17,* 591-620, 1960.

Stommel, H., *The Gulf Stream: A physical and dynamical description,* 2nd ed., 248 pp., University of California Press, Berkeley, 1965.

Svensson, T., Tracer measurement of mixing in the deep water of a small stratified sill fjord, in *Fjord Oceanography,* edited by H. J. Freeland, D. M. Framer, and C. D. Levings, pp. 233-240, Plenum, New York, 1980.

Thorpe, S. A., Experiments on instability and turbulence in a stratified shear flow, *J. Fluid Mech., 61,* 731-751, 1973.

Thorpe, S. A., Transitional phenomena and the development of turbulence in stratified fluids: A review, *J. Geophys. Res., 92,* 5231-5248, 1987.

Toole, J. M., and R. W. Schmitt, Small-scale structures in the north-west Atlantic sub-tropical front, *Nature, 327,* 47-49, 1987.

Toole, J. M., H. Peters, and M. C. Gregg, Upper ocean shear and density variability at the equator during Tropic Heat, *J. Phys. Oceanogr., 17,* 1397-1406, 1987.

Turner, J. S., *Buoyancy Effects in Fluids,* 367 pp., Cambridge University Press, New York, 1973.

Turner, J. S., Turbulent entrainment: The development of the entrainment assumption, and its application to geophysical flows, *J. Fluid Mech., 173,* 431-471, 1986.

Ueda, H., S. Mitsumoto, and S. Komori, Buoyancy effects on the turbulent transport processes in the lower atmosphere, *Q. J. R. Meteorol. Soc., 107,* 561-578, 1981.

Zhang, H., and N. G. Hogg, Circulation and water mass balance in the Brasil Basin, *J. Mar. Res., 50,* 385-420, 1992.

Zilitinkevich, S. S., D. K. Chalikov, and Y. D. Resnyanskiy, Modelling the oceanic upper layer, *Oceanol. Acta, 2,* 219-240, 1979.

G. T. Csanady, Center for Coastal Physical Oceanography, Old Dominion University, Norfolk, VA 23529.

J. L. Pelegrí, Facultad de Ciencias del Mar, Universidad de Las Palmas de Gran Canaria, Campus Universitario de Tafira, 35017 Las Palmas de Gran Canaria, Canary Islands, Spain. (e-mail: pelegri@ciemar.ulpgc.es).

(Received September 18, 1992; revised April 29, 1994; accepted March 28, 1994.)